AGU PUBLICATIONS

Paleoceanography

RESEARCH ARTICLE
10.1002/2016PA003002

Key Points:
- Volume-weighted global benthic $\delta^{18}O$ stack for 0-150 ka on speleothem age model
- Benthic $\delta^{18}O$ responds to insolation with a mean time constant of 3-8 kyr
- Regional stacks allow for diachronous benthic $\delta^{18}O$ change

Supporting Information:
- Supporting Information S1
- Table S1
- Data Set S1
- Data Set S2
- Data Set S3

Correspondence to:
L. E. Lisiecki,
lisiecki@geol.ucsb.edu

Citation:
Lisiecki, L. E., and J. V. Stern (2016), Regional and global benthic $\delta^{18}O$ stacks for the last glacial cycle, *Paleoceanography*, *31*, doi:10.1002/2016PA003002.

Received 8 JUL 2016
Accepted 21 SEP 2016
Accepted article online 23 SEP 2016

Regional and global benthic $\delta^{18}O$ stacks for the last glacial cycle

Lorraine E. Lisiecki[1] and Joseph V. Stern[1]

[1]Department of Earth Science, University of California, Santa Barbara, California, USA

Abstract Although detailed age models exist for some marine sediment records of the last glacial cycle (0–150 ka), age models for many cores rely on the stratigraphic correlation of benthic $\delta^{18}O$, which measures ice volume and deep ocean temperature change. The large amount of data available for the last glacial cycle offers the opportunity to improve upon previous benthic $\delta^{18}O$ compilations, such as the "LR04" global stack. Not only are the age constraints for the LR04 stack now outdated but a single global alignment target neglects regional differences of several thousand years in the timing of benthic $\delta^{18}O$ change during glacial terminations. Here we present regional stacks that characterize mean benthic $\delta^{18}O$ change for 8 ocean regions and a volume-weighted global stack of data from 263 cores. Age models for these stacks are based on radiocarbon data from 0 to 40 ka, correlation to a layer-counted Greenland ice core from 40 to 56 ka, and correlation to radiometrically dated speleothems from 56 to 150 ka. The regional $\delta^{18}O$ stacks offer better stratigraphic alignment targets than the LR04 global stack and, furthermore, suggest that the LR04 stack is biased 1–2 kyr too young throughout the Pleistocene. Finally, we compare global and regional benthic $\delta^{18}O$ responses with sea level estimates for the last glacial cycle.

1. Introduction

The large number of paleoclimate records that exist for the last glacial cycle (0–150 ka) have the potential to greatly improve our understanding of Earth's climate responses on both millennial and orbital time scales. Most notably, this time range covers two glacial terminations and many millennial-scale climate changes. Analysis of paleoclimate records during this time period can yield a wealth of information about climate response times, feedback, stability, and sensitivity to external (orbital) forcing and atmospheric greenhouse gas levels. However, understanding these responses in detail requires high-resolution records of many different parts of the climate system with very precise age control.

Some climate archives are well suited to dating, for example by annual layering or radiometric decay. However, ocean sediment cores are difficult to date precisely despite offering the potential to reconstruct climate responses over more than half of Earth's surface. Radiocarbon offers relatively good age control for the last 40 kyr but is costly and can still have calendar age uncertainties of more than 1000 years due to calibration and reservoir age uncertainty [e.g., *Waelbroeck et al*., 2001; *Stern and Lisiecki*, 2013; *Reimer et al*., 2013]. Beyond 40 ka, sediment cores are generally dated by correlating a paleoclimate proxy to either a better dated climate archive (e.g., ice cores or speleothems) or to changes in Earth's orbital configuration (i.e., "orbital tuning"). The accuracy of stratigraphically correlated age models depends on both the accuracy of the target age model and the extent to which the proxy measured in the core is physically linked to the selected target [*Govin et al*., 2015].

The vast majority of marine sediment cores have age models based on stratigraphic alignment of the oxygen isotope composition ($\delta^{18}O$) of benthic foraminiferal calcite, which measures changes in ice volume and deep ocean temperature. Traditionally, benthic $\delta^{18}O$ has been assumed to change synchronously throughout the ocean despite a 1–2 kyr mixing time for the deep ocean [e.g., *Pisias et al*., 1984; *Imbrie et al*., 1992]. Therefore, a core's benthic $\delta^{18}O$ is often aligned to another core with better age control (e.g., ^{14}C, dated ash layers, or magnetic anomalies) or to a global $\delta^{18}O$ stack (average) [e.g., *Imbrie et al*., 1984; *Lisiecki and Raymo*, 2005]. If $\delta^{18}O$ changes were synchronous, alignment of all records to a single $\delta^{18}O$ target, such as a stack, would allow mutually consistent comparison of the timing of all climate responses recorded in marine sediment cores.

However, radiocarbon age models reveal differences of up to 4 kyr in the timing of benthic $\delta^{18}O$ change during the last glacial termination (T1) [*Skinner and Shackleton*, 2005; *Stern and Lisiecki*, 2014] and likely other late Pleistocene terminations [*Lisiecki and Raymo*, 2009]. Although alignment to a global $\delta^{18}O$ target appears ill

advised during glacial terminations, the timing of $\delta^{18}O$ change may be synchronous to within a few hundred years in certain regions of the ocean bathed by a relatively uniform water mass [*Waelbroeck et al*., 2011; *Stern and Lisiecki*, 2014]. Thus, we develop eight regional benthic $\delta^{18}O$ stacks for the last glacial cycle, which we suggest make better alignment targets than a single global stack. We estimate age differences between regions and account for the considerable uncertainty of these estimated lags. Finally, we construct a volume-weighted global stack for comparison with ice volume (sea level) records and the commonly used "LR04" global benthic stack [*Lisiecki and Raymo*, 2005].

A second goal of this work is to improve the absolute age estimates for $\delta^{18}O$ stratigraphy, accompanied by explicit age uncertainty estimates. The age constraints used in the LR04 stack for the last glacial cycle are now largely outdated. Only one radiocarbon-dated core [*Waelbroeck et al*., 2001] constrains T1, an outdated Greenland ice core age model [*Johnsen et al*., 1992] is used for 20–120 ka, and uncertain coral-based sea level estimates [*Bard et al*., 1990] constrain the penultimate termination (T2). For the new stacks, we use regional radiocarbon compilations from 0 to 40 ka [*Stern and Lisiecki*, 2014], develop millennial-scale correlations between North Atlantic cores, a layer-counted Greenland ice core record from 40 to 56 ka, and radiometrically dated speleothems from 56 to 150 ka. These improved benthic age $\delta^{18}O$ estimates have implications for the entire Pleistocene because the orbital tuning time constant used in the LR04 age model was derived from evaluation of benthic $\delta^{18}O$ responses from 0 to 150 ka.

2. Age Models for the Last Glacial Cycle

2.1. Speleothems

The most precise age models that span the last glacial cycle come from U-series-dated speleothem calcite $\delta^{18}O$ records. Chinese speleothem records are often interpreted as proxies for summer Asian monsoon strength, with more negative values indicating stronger monsoon [e.g., *Wang et al*., 2001]. We created a composite Chinese speleothem record by combining the Hulu and Sanbao records (Figure 1a) with 1.6‰ added to the Sanbao values to correct for fractionation effects due to elevation difference [*Wang et al*., 2008]. The age model for this combined Hulu/Sanbao $\delta^{18}O$ record is constrained by approximately 100 radiometric dates, with age uncertainty less than ±2000 years for the entire interval and around ±100 years (2σ) during T2 due to focused efforts. The pronounced weak monsoon interval (WMI) associated with T2 occurs between 136 and 129 ka [*Cheng et al*., 2009].

Several precisely dated stalagmites are available from caves located at the northern rim of the Alps (NALPS), a region whose climate is tightly coupled with Greenland and the North Atlantic [*Boch et al*., 2011]. Given the more direct climate linkage between the Alps and the North Atlantic and the abrupt changes recorded in the NALPS speleothems, we use these records where available (75–110 ka).

2.2. Greenland Ice Cores

The current reference record for Greenland is North Greenland Ice Core Project (NGRIP) $\delta^{18}O$ [*North Greenland Ice Core Project Members*, 2004] on the layer-counted Greenland Ice Core Chronology 2005 (GICC05) chronology back to 60 ka [*Svensson et al*., 2008] merged with the NGRIP2004 [*North Greenland Ice Core Project Members*, 2004] age model shifted by 750 years from 60 to 122 ka [*Wolff et al*., 2010]. The NGRIP2004 age model is based on correlating to another Greenland ice core back to 105 ka (GRIP on the ss09sea chronology [*Johnsen et al*., 2001]) and to the Antarctic Vostok ice core from 105 to 122 ka [*Petit et al*., 1999]; both of which are derived from ice flow and snow accumulation models. With NGRIP $\delta^{18}O$ on the combined age model (referred to as "GICC05modelext"), light isotopic intervals (stadials) in Greenland consistently occur during heavy isotopic intervals (weak monsoons) in China (Figure 1). Thus, the GICC05modelext and Hulu/Sanbao speleothem age models, which are completely independent, appear to be in excellent agreement over the entire 0–122 ka interval. The North Greenland Eemian Ice Drilling (NEEM) ice core provides an undisturbed section from about 115 to 129 ka, but better absolute age constraints for this core are still needed [*NEEM Community Members*, 2013].

2.3. Antarctic Ice Cores

Recent Antarctic ice core age models are all fixed to GICC05 for 0–60 ka and based on combinations of glaciological modeling and "a wide range of relative and absolute gas and ice stratigraphic markers" [*Veres et al*., 2013] for older portions. The most commonly used Antarctic age models are European Project for Ice

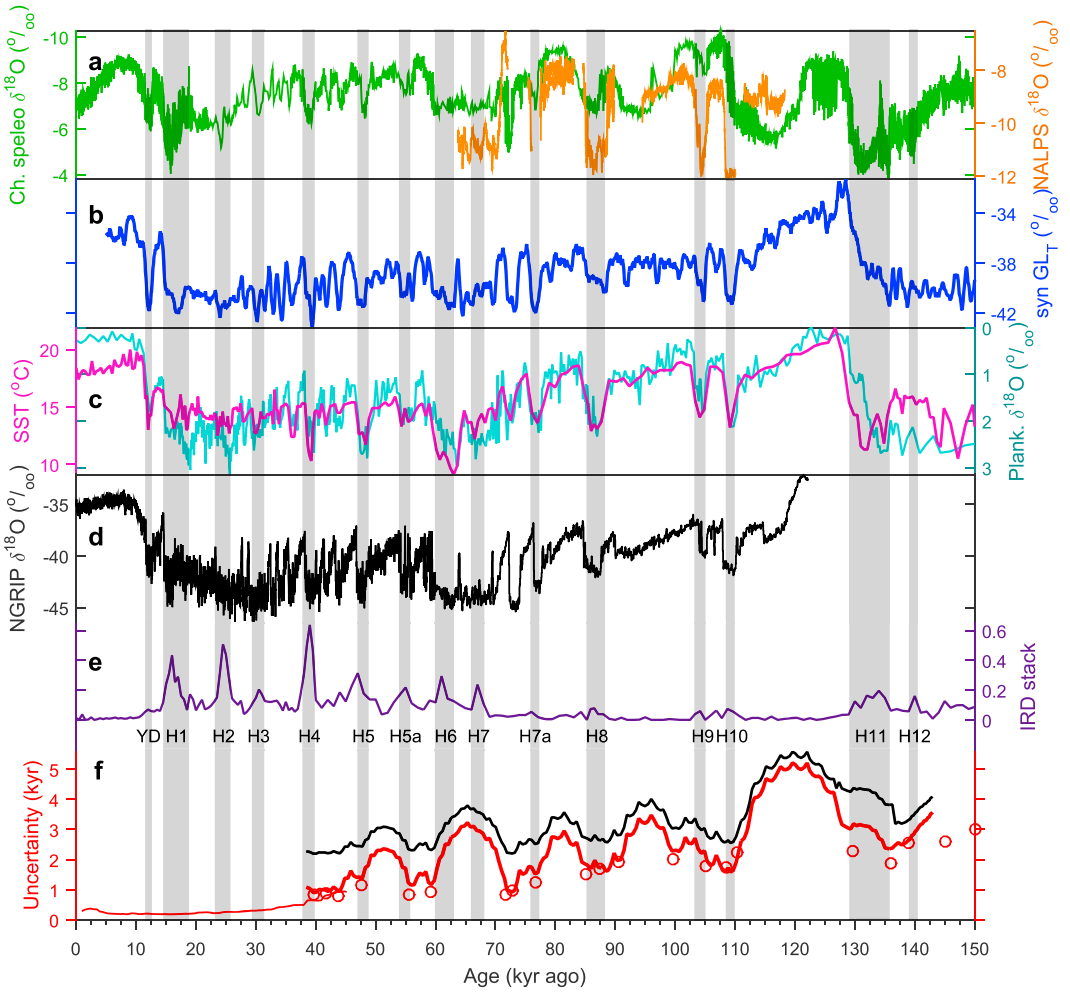

Figure 1. Proxy alignments. (a) Chinese speleothem compilation (green) [*Wang et al.*, 2001, 2008; *Yuan et al.*, 2004; *Cheng et al.*, 2006, 2009; *Wu et al.*, 2009; *Dong et al.*, 2010; *Southon et al.*, 2012] and Alps speleothems (orange) [*Boch et al.*, 2011]; (b) synthetic Greenland temperature (blue) aligned to speleothems [*Barker et al.*, 2011; *Barker and Diz*, 2014]; (c) North Atlantic core MD95-2042 planktonic $\delta^{18}O$ (cyan) [*Shackleton et al.*, 2000] and SST (magenta) [*Pailler and Bard*, 2002] aligned to speleothems; (d) NGRIP ice $\delta^{18}O$, a Greenland temperature proxy, on the GICC05 age model [*North Greenland Ice Core Project Members*, 2004; *Svensson et al.*, 2008; *Wolff et al.*, 2010]; (e) North Atlantic IRD stack (Data Set S1) in arbitrary units; and (f) age uncertainty (half-width of 95% confidence interval) for the deep North Atlantic from radiocarbon (thin red line) [*Stern and Lisiecki*, 2014] and speleothem correlation (circles, thick red line) and for the LS16 global stack (black). The vertical gray bars mark the Younger Dryas (YD) and Heinrich events H1–H12.

Coring in Antarctica (EPICA) Dome C (EDC) 3 [*Parrenin et al.*, 2007], EPICA Dronning Maud Land (EDML) 1 [*Ruth et al.*, 2007], and Antarctic Ice Core Chronology 2012 (AICC2012) [*Bazin et al.*, 2013; *Veres et al.*, 2013]. For the last glacial cycle AICC2012 is by design quite similar to EDC3 and EDML1 and has an uncertainty of less than 2 kyr back to 130 ka and less than 3.5 kyr from 130 to 150 ka.

The AICC2012, EDC3, and EDML1 age models are in good agreement with speleothems and GICC05modelext between 60 and 100 ka. However, AICC2012 ages are 2–3 kyr younger than the corresponding events in Chinese speleothems and in GICC05modelext from ~100 to 120 ka. Over this interval AICC2012 is primarily controlled by low-resolution O_2/N_2 orbital tuning from the Vostok ice core [*Veres et al.*, 2013]. A different O_2/N_2 orbitally tuned age model for the Antarctic Dome Fuji ice core (DFO-2006) [*Kawamura et al.*, 2007] is more consistent with Chinese speleothems and GICC05modelext around 100–120 ka. The DFO-2006 age scale is also about 2 kyr older than AICC2012 from 120 to 140 ka, thus providing two distinct Antarctic age models for T2. One speleothem-correlated Mediterranean sea surface temperature (SST) record matches

the timing of CH_4 change on the AICC2012 age model from 131 to 128 ka [*Marino et al*., 2015], but the best age model for T2 remains uncertain.

2.4. Synthetic Greenland Record

The oldest continuous Greenland ice core is NGRIP (0–122 ka) [*North Greenland Ice Core Project Members*, 2004], and NEEM provides an undisturbed section from about 115 to 129 ka [*NEEM Community Members*, 2013]. *Barker et al*. [2011] calculated a synthetic Greenland $\delta^{18}O$ record that extends beyond these limits, using the longer Antarctic ice core record and assumptions about the thermal bipolar seesaw. The thermal seesaw model accounts for the observed antiphase millennial-scale response in Greenland and Antarctic ice core isotopic records by calling on changes in the Atlantic meridional overturning circulation (AMOC) with an additional heat reservoir to explain the slower warming phases in Antarctica compared to Greenland [*Stocker and Johnsen*, 2003].

Barker et al. [2011] present their synthetic Greenland record on two different age models, EDC3 and SpeleoAge. To create the SpeleoAge age model, the synthetic Greenland record is adjusted to agree with Chinese speleoethem ages. As discussed in the previous section, the largest discrepancy of the past 150 ka between EDC3 and the Chinese speleothems occurs between about 100 and 120 ka, so SpeleoAge is older than EDC3 during this interval. From 0 to 120 ka, SpeleoAge is consistent with Chinese speleothems (by definition), GICC05modelext, and DFO-2006. More recently, *Barker and Diz* [2014] updated SpeleoAge to agree with the timing of NALPS speleothems from 75 to 110 ka (Figure 1b); this age model differs from GICC05modelext by only ~1 kyr. However, SpeleoAge follows EDC3 during T2.

2.5. Sea Level

U-Th-dated corals provide a coherent picture of deglacial sea level changes for T1, with a continuous record documenting the ~130 m rise from 20 to 7 ka [*Carlson and Clark*, 2012; *Lambeck et al*., 2014]. Older portions of the coral-based sea level record are more problematic because (1) U-Th age uncertainties are larger, (2) elevation uncertainty is larger in tectonically active areas because modern uplift/subsidence rates must be extrapolated to the past, and (3) data are generally sparser because of disturbance during subsequent sea level changes. However, age estimates for sea level changes during T2 have been extensively investigated.

Carlson and Winsor [2012] argue that T2 sea level rise probably began between 139 ka, when high-latitude northern hemisphere summer insolation (NHSI) began increasing [*Laskar et al*., 2004], and 137 ka, when Tahiti corals suggest relative sea levels had risen to −85 m [*Thomas et al*., 2009]. Many other coral records show an initial T2 highstand between 135 and 136 ka [*Stein et al*., 1993; *Stirling et al*., 1998; *Esat et al*., 1999; *Gallup et al*., 2002; *Speed and Cheng*, 2004; *Coyne et al*., 2007]. This is consistent with evidence that the Laurentide Ice Sheet began melting by 138 ka ± 3 kyr [*Wood et al*., 2010], and the Scandinavian Ice Sheet began to retreat shortly after 140 ka [*Larsen et al*., 2009].

The beginning of the penultimate sea level highstand, associated with marine isotope stage (MIS) 5e, has age estimates ranging from 126 ka [*Thompson and Goldstein*, 2006; *Waelbroeck et al*., 2008] to 135 ka [*Coyne et al*., 2007]. However, ages around 135 ka are likely associated with a temporary highstand during T2 [*Thomas et al*., 2009]. Coral sea level estimates from the Seychelles islands, which are thought to closely resemble eustatic sea level change, suggest that the sea level highstand was reached by 128.6 ± 0.8 ka [*Dutton et al*., 2015] Thus, the beginning of the interglacial highstand probably began at 128–129 ka [*Chen et al*., 1991; *Stirling et al*., 1998; *Speed and Cheng*, 2004; *Dutton et al*., 2015]. A slightly younger estimate of 126 ka [*Kopp et al*., 2009, 2013] is based on the LR04 age model.

Sea level changes have also been estimated other ways, for example, by separating out the sea level and temperature components affecting foraminiferal $\delta^{18}O$ [e.g., *Bintanja et al*., 2005; *Elderfield et al*., 2012; *Spratt and Lisiecki*, 2016]. Although these methods are less direct indicators of sea level, they provide records with high temporal resolution for portions of the last glacial cycle, where well-dated corals are sparse. In particular, we investigate whether compiled benthic $\delta^{18}O$ records provide support for high-resolution estimates of sea level change in semienclosed basins [e.g., *Grant et al*., 2012; *Rohling et al*., 2014]. These indirect relative sea level estimates have not been corrected for glacial isostatic adjustment and, furthermore, require many assumptions about local temperature and hydrological changes.

3. Age Model Methods

Our basic method was to collect 263 benthic $\delta^{18}O$ records from previous publications (Text S2, Table S1, and Figure S1 in the supporting information), align them to either an Atlantic or Pacific benthic $\delta^{18}O$ target record, and average the data to create regional stacks following the methods of *Stern and Lisiecki* [2014]. We use eight regions: the intermediate North Atlantic, deep North Atlantic, intermediate South Atlantic, deep South Atlantic, intermediate Pacific, deep Pacific, intermediate Indian, and deep Indian. Boundaries for the regions and their volumes are given in Table S2. From 0 to ~40 ka, we use the regional benthic $\delta^{18}O$ stacks and radiocarbon age models of *Stern and Lisiecki* [2014].

Age models for each regional stack beyond 40 ka were developed by correlation with other climate archives. Many different correlations have been used for the last glacial cycle. For example, the age of T2 has been estimated by correlating sea surface temperature (SST) to Antarctic temperature measured in ice cores [*Govin et al*., 2012], ice-rafted debris (IRD) or planktonic $\delta^{18}O$ to Chinese speleothems [*Cheng et al*., 2009; *Caballero-Gill et al*., 2012], North Atlantic SST to an Italian speleothem [*Drysdale et al*., 2009], and Mediterranean planktonic $\delta^{18}O$ to an Israeli speleothem [*Marino et al*., 2015]. Here we use well-documented relationships between North Atlantic climate, Greenland temperature, and Asian weak monsoon intervals (WMIs) [e.g., *Shackleton et al*., 2000; *Wang et al*., 2001; *Cheng et al*., 2009; *Barker et al*., 2011; *Marino et al*., 2015]. Specifically, we correlate (1) a new North Atlantic IRD stack (section 4.2, Data Set S1 in the supporting information) to Asian WMIs and (2) SST and planktonic $\delta^{18}O$ from North Atlantic core MD95-2042 (37.8°N, 10.17°W; 3146 m) [*Shackleton et al*., 2000; *Pailler and Bard*, 2002] to a synthetic Greenland temperature record [*Barker et al*., 2011] with an age model based on Chinese and NALPS speleothem records [*Barker and Diz*, 2014]. These correlations are all mutually consistent (Figure 1) except during T2 when SST lags planktonic $\delta^{18}O$ within core MD95-2042; for this interval we optimize alignment between IRD and the WMI.

Although *Govin et al*. [2015] caution against using an indirect, synthetic record for age model alignment, the SpeleoAge synthetic record provides the best constrained age model spanning the entirety of the last glacial cycle and agrees with available proxy records for Greenland and the North Atlantic region [*Svensson et al*., 2008; *Wolff et al*., 2010; *Boch et al*., 2011; *NEEM Community Members*, 2013]. Thus, the climate hypotheses invoked for our alignment of MD95-2042 are that North Atlantic ice rafting (highest priority) and colder SST on the Iberian margin (weaker priority) are synchronous with cold stadials in Greenland and the northern Alps and with WMIs recorded by Chinese speleothems. Temperature changes in the North Atlantic region and Asian monsoon changes are transmitted via atmospheric processes with lags of less than 1000 years [*Wang et al*., 2008; *Cheng et al*., 2009]; differences between Chinese speleothems are $\leq$1000 years (some of which reflects age model uncertainty) and are visible as apparent noise in Figure 1a. Iceberg movement within the North Atlantic should also be synchronous with Greenland stadials and WMIs to within 1000 years [*Stern and Lisiecki*, 2013].

Age models for other regions are estimated by aligning to MD95-2042 benthic $\delta^{18}O$ with the addition of estimated lags for the deep Indian and deep Pacific regions. Regional $\delta^{18}O$ lags likely always exist due to ocean mixing times [e.g., *Mix and Ruddiman*, 1984; *Broecker et al*., 1988; *Gebbie and Huybers*, 2012]. We estimate constant lags (except during T2) for each region based on present-day ocean circulation and radiocarbon-derived regional age models from 0 to 40 ka [*Stern and Lisiecki*, 2014]. However, lags may vary through time depending on a number of poorly constrained factors (e.g., ocean circulation changes and regions of surface signal "injection"). Therefore, we assign generous uncertainty estimates for these regional lags (see sections 3.3 and 5). Regional age models might be improved in the future by using isotope-enabled circulation models to simulate deepwater temperature and $\delta^{18}O$ signal propagation throughout the ocean in response to millennial- and orbital-scale climate changes.

3.1. Deep North Atlantic Age Model

Our deep North Atlantic age model is based on aligning MD95-2042 planktonic $\delta^{18}O$ [*Shackleton et al*., 2000] to NGRIP $\delta^{18}O$ on the layer-counted GICC05 age model [*North Greenland Ice Core Project Members*, 2004; *Svensson et al*., 2008] for 0–56 ka and aligning the core's alkenone-based SST record [*Pailler and Bard*, 2002] to the synthetic Greenland $\delta^{18}O$ record on an updated SpeleoAge age model [*Barker et al*., 2011; *Barker and Diz*, 2014] for 56–124 ka. Beyond 124 ka we shifted the SpeleoAge age model 2–3 kyr younger to align the timing of Heinrich event 11 IRD with the Asian WMI from 136 to 129 ka [*Cheng et al*., 2009]. This T2 age

adjustment sets a prominent SST cooling at MD95-2042 to 136 ka (Figure 1), similar to the correlation of *Barker et al*. [2011], and sets the rapid planktonic $\delta^{18}O$ decrease to 129 ka, consistent with *Govin et al*. [2012]. Our age range for cold North Atlantic SST during H11 also agrees within uncertainty with ages based on Soreq Cave speleothems from Israel [*Marino et al*., 2015] and the identified "interval of large ice sheet melting" from ~135 to 129 ka in *Govin et al*. [2015].

Marine proxies on the deep North Atlantic age model can be compared with data from ice cores using the Greenland GICC05 age model from 0 to 56 ka and the SpeleoAge Antarctic age model from 0 to 124 ka [*Barker et al*., 2011; *Barker and Diz*, 2014]. (Although stratigraphic correlation was not used for the radiocarbon-dated portion of the stacks, the age model uncertainty of the stacks and GICC05 is sufficiently small from 0 to 40 ka that these age models can be compared with a high degree of confidence.) From 124 to 145 ka, our estimated ages most closely resemble the DFO-2006 ice core age model [*Kawamura et al*., 2007], although we did not specifically use that age model.

3.2. Pacific and Indian Age Models

We extended the Indian and Pacific regional age models beyond the limits of radiocarbon by aligning the benthic $\delta^{18}O$ record of Pacific target core MD97-2120 (45.53°S, 174.93°E; 1210 m) [*Pahnke and Zahn*, 2005] to MD95-2042. This benthic $\delta^{18}O$ alignment allows us to transfer our Atlantic chronology to Indian and Pacific cores (with additional lags for the deep Indo-Pacific). Orbital-scale changes in ice volume and global climate (i.e., responses to greenhouse gas forcing) should have similar effects on benthic $\delta^{18}O$ at these two sites. However, millennial-scale variability may differ due to differences in temperature, hydrologic variability, and meltwater mixing associated with the bipolar seesaw and local-to-regional-scale climate. Therefore, we assign a 2σ uncertainty of 2 kyr to this benthic $\delta^{18}O$ alignment (section 5).

Our correlation of MD97-2120 (hereafter, MD97) to MD95-2042 (hereafter, MD95) is generally similar to the previously published one [*Pahnke et al*., 2003; *Pahnke and Zahn*, 2005] with a few differences (Text S1 and Figures S3 and S4). Alignment of the two benthic $\delta^{18}O$ records suggests many similarities but also some clear differences. Most notably, we align the beginning and end of T2 in MD97 to be synchronous with MD95 because deglacial benthic $\delta^{18}O$ changes begin and end approximately synchronously in the deep North Atlantic and Pacific at ~18 ka during T1 [*Stern and Lisiecki*, 2014]. (Rapid benthic $\delta^{18}O$ change begins ~1 kyr later in the intermediate Pacific, but we choose not to impose this lag on the T2 age model for MD97 because it is also used as the target for the deep Pacific.) Our MD97 alignment in the middle of T2 is similar to the previously published one; smoothing MD97 benthic $\delta^{18}O$ suggests a plateau or slowdown of benthic $\delta^{18}O$ change in the middle of T2 that is not present in MD95. Because we assume that the beginning and end of T2 are synchronous at both sites, differences between the deep North Atlantic and intermediate Pacific regional stacks during T2 do not result from imposed lags. Rather, regional differences in T2 result from the features of their component $\delta^{18}O$ records (e.g., the midtermination plateau) and how each of the individual records aligns with its target core.

After the alignment of MD97 to MD95, a constant lag of 750 years was applied to the deep Pacific and deep Indian regions in approximate agreement with modern deepwater ages [*Gebbie*, 2012]. An additional lag of 2 kyr was also added to the deep Indian stack at the beginning T2 so that it lags the deep Atlantic by ~3000 years at the termination onset. This lag is selected to mimic the delayed onset of T1 in the deep Indian ^{14}C age model [*Stern and Lisiecki*, 2014]. Although the spatial extent of this T1 lag is uncertain [*Stern and Lisiecki*, 2014] and an analogous lag during T2 is speculative, the deep Indian accounts for only 7% of the volume-weighted global stack (Table S2). We investigate the sensitivity of the global stack to the assigned lags with the creation of a maximally coherent "no lag" stack and with Monte Carlo-style sampling of different lags (Figure 2a).

3.3. Age Model Uncertainty

A recent review of last interglacial climate records emphasized the need for systematic quantification of age uncertainties and concluded that the large age uncertainty of ~4 kyr in the LR04 benthic stack represents a significant limitation to the development of accurate age models for marine sediment cores [*Govin et al*., 2015]. Here we quantify age model uncertainty in the deep North Atlantic at tie points based on speleothem age model uncertainty combined with the uncertainty in correlating features between records (Figure 1f and Data Set S2). For portions of the record between explicit tie point, we estimate age uncertainty using the

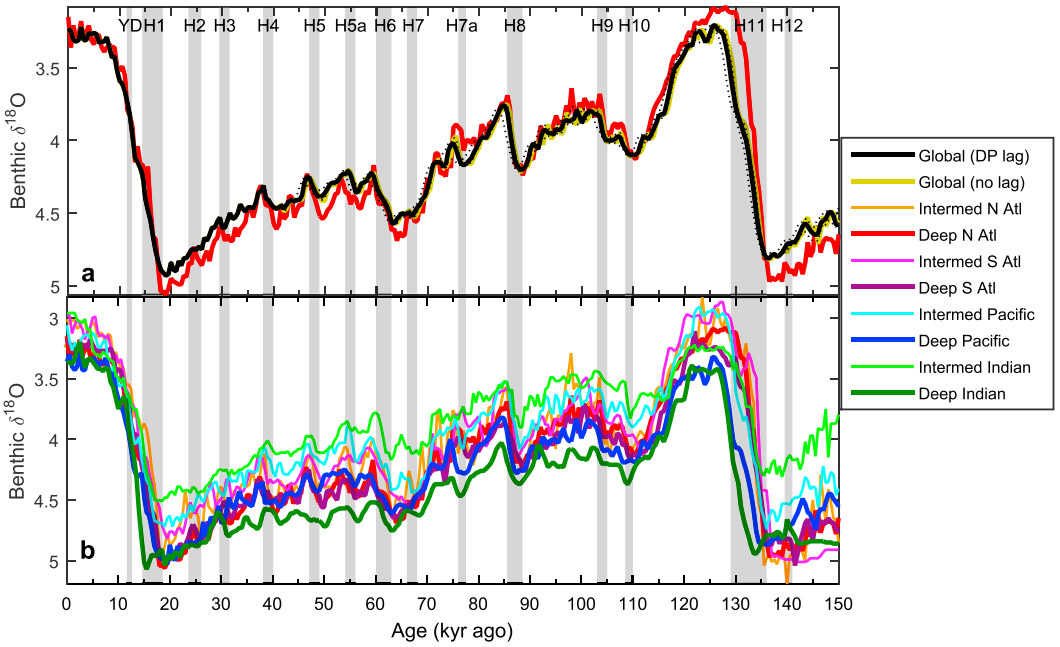

Figure 2. Benthic δ^{18}O stacks. (a) Deep North Atlantic stack (red) compared to volume-weighted global stacks with no regional lags (gold) or with 750 year lags for the deep Pacific and deep Indian (black). The dotted black lines mark the 95% confidence interval based on Monte Carlo-style sampling of different regional lags. (b) All regional stacks with 750 year lags applied to the deep Pacific and deep Indian plus an additional 2000 year lag in the deep Indian at the start of T2.

software Bacon [*Blaauw and Christen*, 2011]. Age uncertainty for the other regional stacks and the global stack includes an additional, independent source of uncertainty to allow for regional differences in the timing of δ^{18}O change. We use a 2σ uncertainty of 2 kyr for regional lags (see section 5) except during T2 (127–136.5 ka), for which we use 3 kyr. When developing age models for new cores, we recommend aligning to the appropriate regional stack and using the global age uncertainty estimates for all regions except the deep North Atlantic.

4. Stacking Methods

4.1. Benthic δ^{18}O

A total of 263 records (Figure S1, Table S1, and Appendix A) contributed to eight regional benthic δ^{18}O stacks. The stacks, their uncertainties, and the number of points and cores per stacked interval are provided in Data Set S3. All Atlantic cores were aligned to MD95-2042, and all Indian and Pacific cores were aligned to MD97-2120. We caution that the millennial-scale features of the resulting stacks may be strongly influenced by these alignment targets because *Stern and Lisiecki* [2014] found variations in stacks' millennial-scale features (but not their terminations) depending upon the alignment target used. However, orbital-scale differences between regions that use the same target (e.g., during MIS 5c in Figure 2b) are likely to reflect real features of the data.

We aligned 164 Atlantic benthic δ^{18}O records to MD95-2042 benthic δ^{18}O on our age model (section 3.1) using the automated alignment software Match [*Lisiecki and Lisiecki*, 2002]. Four regional Atlantic stacks were constructed by averaging together available δ^{18}O data points within each region, consistent with the method of *Stern and Lisiecki* [2014]. The deep North Atlantic stack has a resolution of 500 years and is the average of all available aligned benthic δ^{18}O values within ±250 years. The other Atlantic stacks have a smoothed 500 year resolution, with each stacked point being the average of available benthic δ^{18}O values within ±500 years.

All Pacific and Indian benthic δ^{18}O records were aligned to MD97-2120, which was aligned to Atlantic core MD95-2042 as described in section 3.2. We applied a constant 750 year lag to the deep Indian and deep Pacific (see section 5) and an additional lag of 2000 years to the start of T2 in the deep Indian to match the

response observed during T1 using ^{14}C age models [*Stern and Lisiecki*, 2014]. Then we calculated a stack value for each region every 500 years. The intermediate Pacific stack has a stacked point every 500 years that is the average of all available regional benthic $\delta^{18}O$ records within ±500 years. The deep Pacific stack has a "true" 500 year resolution (stacked point every 500 years that is the average of points within ±250 years) for 0–40 ka, but from 40.5 to 145 ka has a smoothed 500 year resolution that averages points within ±500 years. In the deep Indian stack, each point averages data within ±500 years from 0 to 40.5 ka and ±1000 years from 41 to 145 ka. Likewise, the intermediate Indian stack, which contains only three cores, has a stacked point every 500 years that averages data within ±1000 years.

Adjusting the amount of smoothing over the lengths of the stacks is necessary because the amount of data constraining the stacks decreases with age. We chose to have a stacked point every 500 years in all the stacks so we could compare and combine them without interpolation. However, even with taking the average of points within ±1000 years, the intermediate Indian stack contains no data from 0 to 1 ka and at 76.5 ka and the deep Indian contains no data from 144 to 145 ka. We copied neighboring values in the stacks to fill in these empty stacked values in order to generate the volume-weighted global stack. Additional caution should be taken when considering the youngest and oldest few thousand years of these stacks. Where the regional stacks were constrained by zero to one core, we assigned a $\delta^{18}O$ uncertainty estimate of 0.3‰ (1σ).

For 0 to ~40 ka, we use the radiocarbon-dated regional stacks of *Stern and Lisiecki* [2014]. The exact age of transition between the previously published data and the new data varies to ensure consistency across the transition. Regional radiocarbon stacks are used back to 40.5 ka in the deep Indian, 40 ka in the deep Pacific, 38 ka in the intermediate Pacific, and 39 ka in all four Atlantic stacks. *Stern and Lisiecki* [2014] did not create a stack or age model for the intermediate Indian because only one radiocarbon-dated record was available [*Sarnthein et al*., 2011]. However, that ^{14}C record plus one from 2100 m suggests that the very late onset of T1 in the deep Indian did not affect intermediate depths [*Waelbroeck et al*., 2006]. Therefore, we assume that the intermediate Indian responses were synchronous with the intermediate Pacific ^{14}C age model from 0 to 38 ka.

Finally, all eight regional stacks were volume weighted (Table S2) and averaged to produce a global stack, hereafter referred to as the "LS16" global stack (Data Set S3).

4.2. IRD

We extended the IRD stack of *Stern and Lisiecki* [2013] back to 150 ka using the same 15 records (Data Set S1 and Figure S2). From 0 to 40 ka, the IRD stack has 500 year resolution and a deep North Atlantic radiocarbon age model [*Stern and Lisiecki*, 2013]. The new 40–150 ka portion of the stack has 1000 year resolution and is dated by correlation to GICC05 and speleothem age models (Figure 1). Other than switching to lower resolution, the IRD records and stacking methods are the same as those presented in *Stern and Lisiecki* [2013].

We identify a series of 15 IRD peaks labeled as Heinrich events (H#), with the following caveats about nomenclature. *Heinrich* [1988] originally identified a series of 11 correlative IRD events, H1–H11. H0 was subsequently identified in the Younger Dryas [e.g., *Skinner et al*., 2003]. H5a, occurring before GI-14, is another well-established event [*Rashid et al*., 2003], although not recognized by *Heinrich* [1988]. H7–10 are less commonly used for stratigraphic purposes because they are generally minor peaks that occurred before full glacial conditions. *Channell et al*. [2012] identified distinct H7 and 7a peaks, and we follow their definitions. H8 occurred during MIS 5b and H10 during MIS 5d [*Heinrich*, 1988]. The stratigraphic position of H9 is not well established, but a minor peak around 105 ka from a single core makes an obvious candidate because it also lines up with significant features in other paleoclimate records (Figure 1). H11 is well known to have occurred during T2 [e.g., *McManus et al*., 1999]. Although *Heinrich* [1988] stopped with H11, we extend the naming convention to H12 for a peak at 140 ka, which corresponds to "H6.2" of *Channell et al*. [2012].

5. Constraints on Regional Lags in Benthic $\delta^{18}O$

Regional ^{14}C age models yield estimates of regional differences in the timing of T1 [*Stern and Lisiecki*, 2014]. However, the relative scarcity of data from the Indian and Pacific oceans yields larger uncertainties about the variability in the timing of T1 within these regions (e.g., differences with respect to latitude or depth within the deep Pacific). The ^{14}C age models also provide relatively little information about the regional phase lags

before T1 because millennial-scale variability reconstructed in the regional stacks from 25 to 40 ka is highly dependent upon the choice of alignment target [*Stern and Lisiecki*, 2014].

Several factors indicate that for most locations, regional benthic $\delta^{18}O$ lags are likely to be less than 2 kyr except during terminations. First, only one region (the deep Indian Ocean) exhibits a benthic $\delta^{18}O$ lag larger than 2 kyr during T1 and that lag occurs in conjunction with very weak Atlantic meridional overturning circulation (AMOC) during H1. Throughout most of the last glacial cycle, the AMOC is likely significantly stronger than during H1 [e.g., *McManus et al*., 2004; *Böhm et al*., 2015]. Second, benthic $\delta^{18}O$ changes of 0.2–0.3‰ are observed throughout the deep ocean during multiple Heinrich events (Figure 2b). Given that the repeat time for these events is 5–7.5 kyr, their amplitudes would not be well preserved if the $\delta^{18}O$ signals took more than ~2 kyr to propagate through most of the ocean. Third, a tracer transport model indicates that a globally uniform surface signal would take only 1175 years to reach the deep Pacific, producing an 800 year lag between the deep Atlantic and deep Pacific [*Gebbie*, 2012]. However, longer lags are needed to reach benthic $\delta^{18}O$ equilibrium [*Wunsch and Heimbach*, 2008] or if tracers are injected into the surface ocean only in specific regions [*Siberlin and Wunsch*, 2011].

Fourth, the assumption of synchronous benthic $\delta^{18}O$ change between the deep Atlantic and intermediate Pacific produces estimated ages for the Pacific Toba tephra of 73.8 ka in MD97-2151 [*Wei et al*., 2006] and at 74.2 ka in GIK17961 [*Bühring et al*., 2000] (Figure S3), in excellent agreement with radiometric ages of 73.88 ka ± 0.32 kyr [*Storey et al*., 2012]. This suggests an intermediate Pacific lag of less than 400 years. Collectively, these lines of evidence support a 2σ age uncertainty of 2 kyr for regional differences in the timing of benthic $\delta^{18}O$ change except during terminations (for which we use 3 kyr).

To quantify the potential effects of different regional lags on the volume-weighted global stack, we generate a maximally coherent stack with no regional lags and perform Monte Carlo-style sampling of different regional lags (Figure 2). To estimate reasonable potential lags between regions, we assume that the benthic $\delta^{18}O$ stack of the deep North Atlantic likely represents deep water with an age of ~500 years [*Gebbie*, 2012]. Then we apply age shifts for other regions relative to the deep North Atlantic. The intermediate North Atlantic is assumed to remain synchronous with the deep North Atlantic. The intermediate South Atlantic, deep South Atlantic, and intermediate Indian regions are allowed to vary between a lead of 500 years and a lag of 500 years. For the intermediate Pacific we simulate lags of 0–1000 years based on a ^{14}C-estimated lag of 1000 years during the onset of T1 [*Stern and Lisiecki*, 2014]. The deep Pacific and the deep Indian stacks are simulated to lag the deep Atlantic by 0–2000 years. Although we do not explicitly simulate a larger deep Pacific lag during the termination, the no lag deep Pacific stack actually has a lag of ~3000 years in the middle of T2 due to the midtermination plateau (section 3.2 and Figure 2b).

For each Monte Carlo sample, time-varying regional lags were generated using first-order autoregressive random walks with time steps of 500 years. The lag at time step t (lag_t) is generated as $0.99\ lag_{t-1} + 0.01\ X_t$, where X is the normalized Gaussian white noise. One random walk was scaled to a minimum −500 years and a maximum of +500 years and applied to the intermediate South Atlantic, the deep South Atlantic, and the intermediate Indian stacks. Another random walk was scaled to a minimum of 0 year and a maximum of 2000 years and applied to the deep Pacific and deep Indian stacks. The intermediate Pacific lag is assigned to be half the deep Pacific lag. Finally, the time-shifted regional stacks were combined to produce a volume-weighted global stack. This sampling was repeated 1000 times. The mean of the 1000 sample global stacks is similar to (but slightly smoother than) the LS16 global stack, which uses a constant 750 year lag for the deep Indo-Pacific. The 95% confidence interval for the global stack (estimated from our 1000 samples) has an upper bound that is similar to the no lag stack and a lower bound that is approximately consistent with the LS16 stack lagged by an additional 1000 years (Figure 2a and Data Set S3).

6. New Global Stack Compared to LR04

The basic features of the volume-weighted LS16 global stack and the LR04 global stack [*Lisiecki and Raymo*, 2005] are similar but with some notable differences particularly in their age models (Figure 3a). LS16 is based on over 5 times as many records as LR04 for the last glacial cycle (48 versus 263). Volume weighting the regional stacks in LS16 also prevents the Atlantic bias found in LR04 caused by a greater number of cores from the Atlantic than Pacific. While LR04 is based on the assumption of globally synchronous benthic $\delta^{18}O$ changes

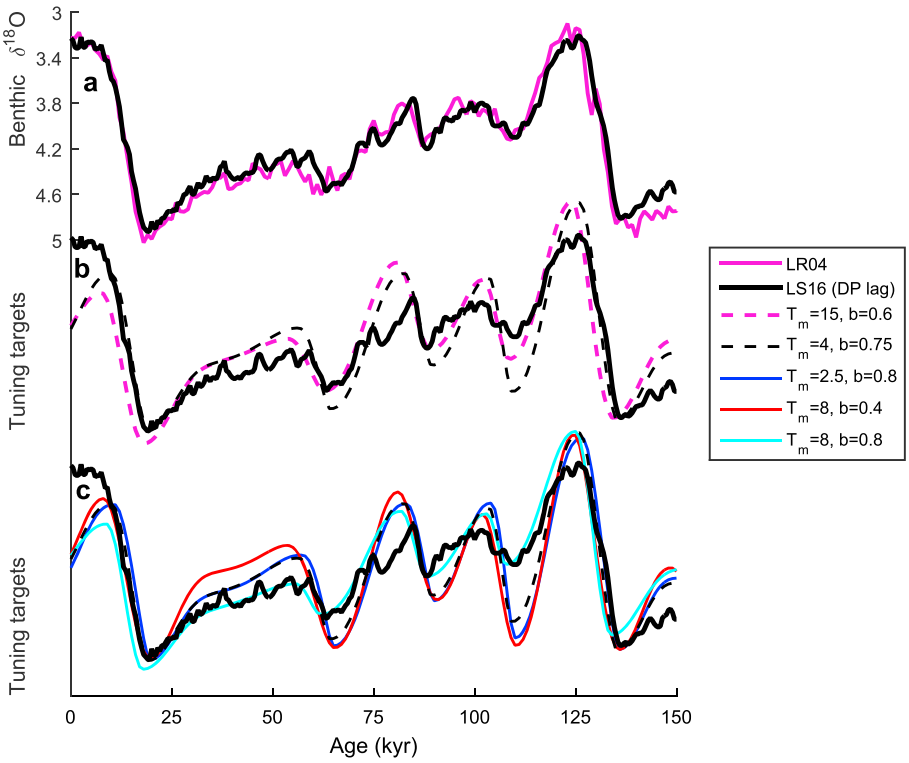

Figure 3. Benthic δ^{18}O age models. (a) LS16 volume-weighted global benthic δ^{18}O stack (black) and LR04 stack (magenta) [*Lisiecki and Raymo*, 2005]. (b) Tuning targets [*Imbrie and Imbrie*, 1980] with mean time constants of 15 kyr (dashed magenta, as used in *Lisiecki and Raymo* [2005]) and 4 kyr (dashed black) as optimized to fit the LS16 global stack. (c) Sensitivity test comparing LS16 global stack with model results for alternate parameter values.

for its entire length, LS16 assumes a lag 750 years for the deep Pacific and deep Indian, with larger lags during T2. Age uncertainty in the new global stack ranges from 2200 to 4000 years for 38–112 ka (Figure 1f), whereas uncertainty for the late Pleistocene portion of LR04 is qualitatively estimated to be 4 kyr. From 113 to 127 ka, age uncertainty in the LS16 stack is ~5000 years, primarily due to the lack of distinctive features for stratigraphic correlation in the North Atlantic during MIS 5e.

During T2 the LS16 global stack leads LR04 by 1–2 kyr; however, the regional stacks vary greatly. Whereas T2 spans 137–126 ka in LR04, we estimate that T2 occurred from 137 to 130 ka in the deep North Atlantic and 133–127 ka in the deep Indian. Therefore, correlations to LR04 may differ from the new regional age models by up to 4 kyr during either the beginning or end of T2, depending on core location. The relative timing of Atlantic and Pacific benthic δ^{18}O during T2 in our stacks is remarkably similar to earlier results from *Lisiecki and Raymo* [2009] based on sedimentation rates. *Lisiecki and Raymo* [2009] found an ~4000 year Atlantic-Pacific lag at the end of T2 and a smaller ~1500 year maximum lag during T1. Similarly, radiocarbon age models suggest an ~1500 year lag for T1 [*Stern and Lisiecki*, 2014], and our regional stacks suggest a 3000–4000 year lag during T2 due to a midtermination plateau in deep Pacific benthic δ^{18}O (Figure 3b). However, the new Atlantic and Pacific regional stacks are both older at T2 than their counterparts in *Lisiecki and Raymo* [2009]. Our new regional age estimates for T2 are also in good agreement with age models for MD95-2042 and the Indian sector of the Southern Ocean estimated based on SST alignments to ice core records [*Govin et al*., 2015]. The MIS 5e plateau in the LS16 global δ^{18}O stack begins at 127.5 ka, approximately synchronously with the start of the sea level highstand (section 2.5).

LS16 is up to 2000 years older than LR04 during MIS 5e and 5d. The Atlantic regional stacks, which resemble LR04 during this interval, display a more gradual transition than the Pacific stacks. A rapid MIS 5e/5d transition occurs in the Pacific target core MD97-2120 using either our age model or *Pahnke and Zahn* [2005]. A compilation of high-resolution benthic δ^{18}O records also shows this characteristic rapid end to MIS 5e in the Pacific and a more gradual 5e/5d transition in the Atlantic [*Govin et al*., 2009]. We conclude that

Atlantic benthic $\delta^{18}O$ increases gradually from 122 to 111 ka, whereas Pacific benthic $\delta^{18}O$ increases rapidly from 119 to 116 ka, followed by an additional step-like increase at 111–112 ka. The response in the LS16 global stack falls between these two. A relatively early MIS 5e/5d transition in our Pacific stacks generates a global stack similar to a speleothem-based age model North Atlantic age model [*Hodell et al*., 2013] but a Pacific MIS 5e plateau that is ~3000 years longer than the speleothem-based age model for a South China Sea core (Figure S5) [*Caballero-Gill et al*., 2012]. Overall, the regional and global benthic $\delta^{18}O$ changes are in good agreement with the identification of glacial inception globally from 122 to 113 ka and "glacial conditions" from 113 to 106 ka [*Govin et al*., 2015].

LS16 shows a clear two-step decrease from MIS 5d into 5c, coeval with H9 and H10, whereas this detail was smoothed in the lower-resolution LR04 stack. The LR04 stack has a decreasing trend over MIS 5c; the LS16 global stack generally increases, but the shape of MIS 5c varies greatly among the regional stacks (Figure 2b). Most intermediate-depth regions show a broad plateau from 93 to 108 ka, while most deep regions exhibit depleted $\delta^{18}O$ peaks at 100 and 102 ka. However, a late peak is observed at 92.5 ka in the deep Indian, and the most depleted values for all of MIS 5c are observed at 98 ka in the intermediate North Atlantic. Thus, the regional stacks suggest great spatial variability in temperature (or hydrologic cycle) changes during MIS 5c.

The MIS 5a peak at 85 ka is slightly earlier than in LR04 and synchronous with the end of H8, the onset of GI-21, and a CO_2 peak in Byrd ice core [*Ahn and Brook*, 2008] on the AICC2012 chronology. However, correspondence between LR04 and LS16 is excellent during transition from MIS 5a to 4. Millennial-scale benthic $\delta^{18}O$ peaks at 72 and 75 ka are coeval with the onsets of GI 19 and 20, respectively, and their associated CO_2 peaks.

Maximum values for MIS 4 occur between 67 and 63 ka in the LS16 stack as bound by H7 and GI-18 and are 2–3 kyr earlier than in LR04. The light $\delta^{18}O$ peak in the middle of MIS 4 in LR04 is less pronounced in the LS16 global stack but well resolved in the intermediate Pacific and intermediate Indian regions (Figure 2b). During MIS 3, millennial-scale benthic $\delta^{18}O$ variability in LS16 is older than LR04 by up to 4 kyr as a result of switching from the GRIP age model [*Johnsen et al*., 1992] to GICC05 [*Svensson et al*., 2008]. The two stacks are in better agreement near H4 due to the long-standing age constraint provided by the Laschamp magnetic excursion at ~41 ka [e.g., *Laj et al*., 2000].

From 0 to 39 ka the LS16 stack uses regional ^{14}C age models [*Stern and Lisiecki*, 2014]. LS16 contains a millennial-scale peak associated with H4 at 38 ka that is nearly identical to one in LR04. However, there is no obvious analog for the peak at 26 ka in LR04; instead, LS16 contains a modest global peak at 29.5 ka following H3 and regional Atlantic peaks at 24.5 ka during H2. The timing of T1 is very similar in LR04 and LS16; rapid benthic $\delta^{18}O$ decrease begins at 18 ka in both. The rate of change decreases briefly in LS16 from 13 to 14 ka due to midtermination plateaus in many of the regional stacks, particularly the intermediate and deep Pacific. The end of T1 is easily identifiable at 7.5 ka in LS16, whereas LR04 benthic $\delta^{18}O$ gradually decreases throughout most of the Holocene.

7. Orbital Tuning Implications

Collectively, age differences between the LS16 and LR04 global stacks suggest an error in the benthic $\delta^{18}O$ response time used to set the lag between insolation and the LR04 stack throughout the Pleistocene (Figure 3). Orbital tuning in the LR04 global stack is based on alignment to a simple, two-parameter model [*Imbrie and Imbrie*, 1980],

$$\frac{dy}{dt} = \frac{1 \pm b}{T_m}(x - y)$$

where x is the normalized insolation [*Laskar et al*., 2004], y is the modeled climate response, T_m is the mean time constant of the system, and b is a nonlinearity coefficient that is subtracted during ice growth and added during ice retreat. *Lisiecki and Raymo* [2005] selected values of $T_m = 15$ kyr and $b = 0.6$ for 0–1.5 Ma based on optimizing model agreement with age constraints for benthic $\delta^{18}O$ change over the last glacial cycle. Thus, the age model of our new stack may have implications for a large portion of the LR04 age model.

Although *Imbrie and Imbrie* [1980] designed their model to emulate the tendency of ice sheets to shrink faster than they grow, the authors only refer to y as an unspecified "climatic response." In fact, when used as a

tuning target for benthic $\delta^{18}O$, the model output y implicitly includes the combined responses of both ice volume and deepwater temperature. Temperature may represent 40% or more of the total benthic $\delta^{18}O$ signal and likely changes faster than ice volume [e.g., *Bintanja et al*., 2005; *Shakun et al*., 2012, 2015; *Spratt and Lisiecki*, 2016]. Thus, the value of T_m that best simulates the response of benthic $\delta^{18}O$ could be significantly smaller than the mean physical response time of the Laurentide ice sheet. However, the response time of benthic $\delta^{18}O$ may still be considered indicative of high-latitude climate change, which is the dominant factor affecting both ice volume and deepwater temperature [e.g., *Bintanja et al*., 2005].

Other models of late Pleistocene glacial cycles may describe the nonlinear dynamics of the climate system more realistically than the *Imbrie and Imbrie* [1980] model [e.g., *Parrenin and Paillard*, 2012; *Garcia-Olivares and Herrero*, 2013; *Abe-Ouchi et al*., 2013], but there is not yet consensus on which model is best or how to simulate changes in glacial dynamics across the mid-Pleistocene transition at 800 ka. Also, small changes to the parameter values used in these models can result in dramatically different predictions for the timing of glacial terminations. We use the *Imbrie and Imbrie* [1980] model because it is easily computed, relatively insensitive to small changes in parameter values, reproduces many features of late Pleistocene benthic $\delta^{18}O$ record, and can potentially be used throughout the Pliocene-Pleistocene by applying simple parameter changes [*Raymo et al*., 2006].

The model parameters used for LR04 ($T_m = 15$ kyr, $b = 0.6$) produce warming responses which are too young compared to T2 and the start of MIS 3 in the LS16 global stack (Figure 3). To find the parameter values which best fit the LS16 stack, we visually compared a wide variety of parameter pairs with the data. The simple form of the *Imbrie and Imbrie* [1980] model makes it relatively straightforward to assess the effects of changes in both T_m and b. We qualitatively identify the best fit to be produced by $T_m = 4$ and $b = 0.75$ (Figure 3). However, model results are relatively insensitive to small changes in T_m and b; T_m values of 3–8 kyr can be made to agree with the LS16 stack if b is adjusted accordingly. In Figure 3c we show models at the limits of what we consider to be an acceptable fit. A T_m value as small as 2.5 kyr ($b = 0.8$) fits the stack reasonably well except for responses that are too early during T1 and the end of MIS 5e. A T_m value as large as 8 kyr ($b = 0.4$) also fits reasonably well. Pairing $T_m = 8$ with a larger nonlinearity coefficient (e.g., $b = 0.8$) underestimates ages for the start of MIS 3 and $\delta^{18}O$ maxima at MIS 4 and 5d.

The mean response time of benthic $\delta^{18}O$ throughout the Pleistocene is unlikely to be much larger than the observed responses from 0 to 150 ka. Whereas LR04 gradually increased T_m from 5 to 15 kyr from 3 to 1.5 Ma and then held T_m constant at 15 kyr from 1.5 to 0 Ma, alternate tuning targets could be created that use a T_m of 4–8 kyr for 3–0 Ma (along with corresponding b values). These new tuning targets would make the LR04 stack 1–2 kyr older from 0.15 to 1.5 Ma and ~1 kyr older from 1.5 to 3 Ma. These age adjustments would also make the phase lags of Pleistocene climate proxies estimated using the LR04 age model smaller by ~20° relative to orbital precession, ~14° relative to obliquity, and ~6° relative to eccentricity. Thus, a variety of Pleistocene climate changes (e.g., SST and overturning circulation) may respond more rapidly to insolation than previously estimated [e.g., *Lisiecki et al*., 2008; *Sosdian and Rosenthal*, 2009; *Shakun et al*., 2015].

8. Comparison of Benthic $\delta^{18}O$ and Sea Level

8.1. Terminations

Although benthic $\delta^{18}O$ is affected by ice volume, deepwater temperature, and changes in the hydrologic cycle (i.e., the relationship between salinity and seawater $\delta^{18}O$), benthic $\delta^{18}O$ is often interpreted as an ice volume (sea level) proxy, either through simple scaling (see discussions in *Duplessy et al*. [2002] and *Siddall et al*. [2008]) or more sophisticated inverse modeling [*Bintanja et al*., 2005]. From the Last Glacial Maximum (LGM) to Holocene, the ice volume contribution to the global mean seawater $\delta^{18}O$ change was 1.05 ± 0.2‰ [*Adkins et al*., 2002; *Duplessy et al*., 2002]. The LGM-Holocene difference (maximum-minimum values) in LS16 is 1.71 ± 0.013‰, similar to the magnitude of T1 in LR04 (1.78 ± 0.10‰). Thus, 50–75% of the T1 decrease in LS16 are due to ice volume, with the remainder caused by warming and/or hydrologic cycle changes. This proportion probably changed with time, but quantitative constraints are limited [*Bintanja et al*., 2005; *Spratt and Lisiecki*, 2016].

Despite a significant temperature component in the benthic $\delta^{18}O$ signal, the LS16 age model supports similar timing (within ~2 kyr) for changes in global mean benthic $\delta^{18}O$ and global mean sea level during

terminations. Although portions of the Laurentide ice sheet began to retreat at 23 ka [*Ullman et al*., 2015], global sea level rise is estimated to have begun between 20.5 and 19 ka [*Clark et al*., 2009; *Lambeck et al*., 2014], followed by an initial decrease in mean benthic δ^{18}O at 18.5 ka. However, benthic δ^{18}O leads sea level by 500–1000 years for most of the termination, likely because deep ocean temperature warmed more quickly than ice sheets retreated [*Elderfield et al*., 2010]. The Holocene benthic δ^{18}O plateau begins at 7.5 ka, approximately synchronous with the beginning of the sea level highstand at 7 ka [*Smith et al*., 2011; *Lambeck et al*., 2014]. The beginning and end of T2 in the LS16 stack are fairly well constrained by the Asian WMI during H11. The end of T2 in LS16 occurs at 127.5 ka, ~1000 years after the start of the sea level highstand at 128.6 ± 0.8 ka [*Dutton et al*., 2015]. A similar comparison between sea level rise and δ^{18}O change at the start of T2 is complicated by disagreement between sea level studies [e.g., *Drysdale et al*., 2009; *Grant et al*., 2012].

Here we use the similarities between sea level and δ^{18}O change during T1 to suggest that the timing of δ^{18}O change at the beginning of T2 could provide an independent test of T2 sea level reconstructions with an uncertainty of ~2 kyr. If the relative timing and proportion of the ice volume, temperature, and hydrologic cycle contributions to benthic δ^{18}O were similar for both T1 and T2, the scaling between sea level and global (or regional) benthic δ^{18}O change could be used as a method to estimate the timing of sea level change during T2. Because our benthic δ^{18}O age models are based on correlation between North Atlantic IRD and Chinese speleothems, this technique is independent of other T2 dating techniques, which have produced estimates of 141 to 130.5 ka for the termination onset [*Drysdale et al*., 2009; *Thomas et al*., 2009; *Sarnthein et al*., 2013].

Global benthic δ^{18}O changes by 0.008–0.009‰ per meter of sea level change during T1 [*Clark et al*., 2009] with age offsets of approximately ±1000 years. At the beginning of T2, the LS16 global stack decreases by only 0.10‰ at 135 ka, which is equivalent to 11–12.5 m of sea level rise assuming constant deepwater temperature. The no lag global stack produces a slightly higher estimate of 0.13‰ change at 135 ka, equivalent to 14–16 m of sea level rise. (Maximum δ^{18}O values are observed in both global stacks at 136.5 ka.) Based on these relationships, it would be nearly impossible to accommodate >40 m of deglacial sea level rise by 137 ka as previously proposed [*Drysdale et al*., 2009; *Thomas et al*., 2009]. Potential caveats are that we make no explicit estimate of eustatic sea level at the beginning of T2 (see section 8.2), and benthic δ^{18}O cannot identify sea level rise accompanied by deepwater cooling (e.g., ~1°C to mask 30 m of sea level rise), which is unlikely to occur during terminations.

An alternative way to estimate sea level change would be using only the deep North Atlantic stack, which has a T2 age model with smaller error bars based on direct correlation between IRD and Chinese speleothems. However, in the first part of a termination, deep North Atlantic δ^{18}O change is highly amplified relative to the global mean by some combination of unevenly mixed meltwater input, temperature change, and circulation change [e.g., *Skinner et al*., 2003; *Waelbroeck et al*., 2011]. We make no attempt to deconvolve these contributions (although see *Skinner and Shackleton* [2006]). Instead, we assume that the response of deep North Atlantic benthic δ^{18}O to a given amount of freshwater input may be similar during both H1 and H11 because similar mechanisms appear to operate during both events (section 9). Thus, we develop an empirical scaling between the deep North Atlantic stack and eustatic sea level of −0.75‰ = +30 m based on changes during H1 (19.5–15 ka) [*Clark et al*., 2009; *Stern and Lisiecki*, 2014]. At the beginning of T2, the deep North Atlantic stack changes by −0.43‰ at 135 ka (95% confidence interval: 132.5–137.5 ka), which would correspond to ~17 m of sea level rise. This timing estimate for T2 ice volume change agrees with other recent reconstructions [*Carlson and Winsor*, 2012; *Grant et al*., 2012; *Govin et al*., 2015] and is consistent with forcing from increased NHSI (21 June) beginning at 139 ka (Figure 4).

8.2. Millennial-Scale Variability

Heinrich events during MIS 5 and MIS 3 are associated with decreases in benthic δ^{18}O (Figure 2). Benthic δ^{18}O changes of 0.2–0.4‰ are observed in all regions for H4–6 and H7a–10, with the largest amplitudes in the intermediate North Atlantic and intermediate Pacific. Decreasing benthic δ^{18}O values are consistent with reduced ice volume [*Clark et al*., 2007; *Sierro et al*., 2009], possibly accompanied by intermediate-depth warming [*Clark et al*., 2007; *Marcott et al*., 2011] or brine-generated deep water [*Waelbroeck et al*., 2011]. Additionally, millennial-scale benthic δ^{18}O variability at MD95-2042 and other Iberian Margin sites has been associated with shifts between northern and southern source deep water [e.g., *Skinner et al*., 2003; *Skinner*

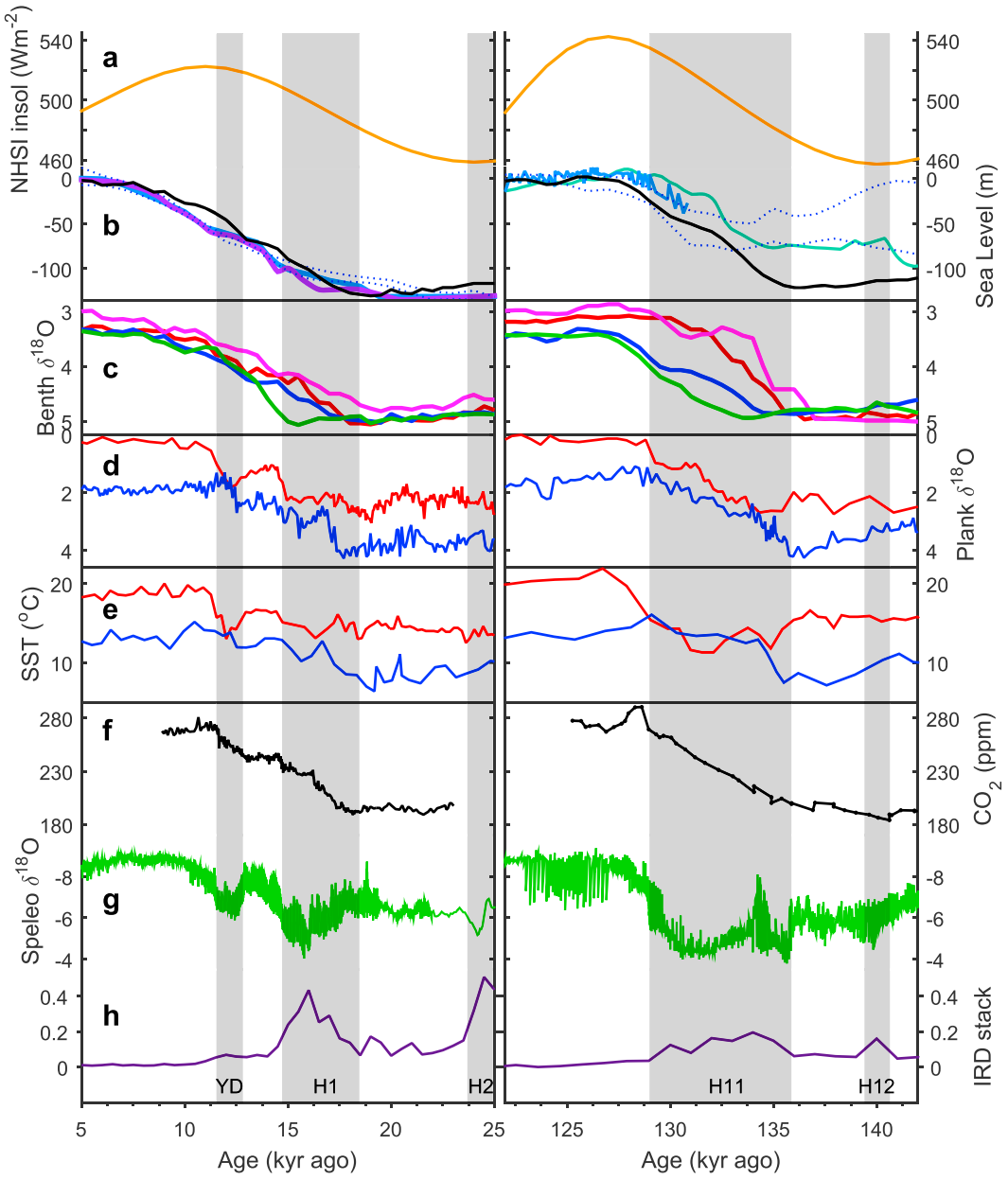

Figure 4. Comparison of (left) T1 and (right) T2. (a) The 21 June insolation at 65°N [*Laskar et al.*, 2004]. (b) Eustatic sea level for T1 (blue: *Clark et al.* [2009]; purple: *Lambeck et al.* [2014]) and T2 (blue: *Kopp et al.* [2009] after conversion from LR04 to LS16 age model). Coral-based sea level 95% confidence range (dotted black) [*Medina-Elizalde*, 2013] and Red Sea relative sea level (teal) [*Grant et al.*, 2012]. For comparison, the LS16 global stack (black) is scaled based on T1 change (1.7‰ = 130 m). (c) Regional benthic $\delta^{18}O$ stacks for the intermediate South Atlantic (pink), deep North Atlantic (dark red), deep Pacific (blue), and deep Indian (green). (d) Planktonic $\delta^{18}O$ from North Atlantic core MD95-2042 (red) [*Shackleton et al.*, 2000] and South Pacific core MD97-2120 (blue) [*Pahnke et al.*, 2003]. (e) SST from MD95-2042 (red) [*Pailler and Bard*, 2002] and MD97-2120 (blue) [*Pahnke et al.*, 2003]. (f) Atmospheric pCO_2 [*Marcott et al.*, 2014; *Landais et al.*, 2013]. (g) Chinese speleothem data as in Figure 1a. (h) IRD stack and Heinrich event labels as in Figure 1e.

and Elderfield, 2007], but this mechanism is regional rather than global. The amount of sea level change associated with millennial-scale variability during MIS 3 is estimated by models and data to be about 10 m [*Clark et al.*, 2007; *Grant et al.*, 2012]. Heinrich events are expected to occur midway through periods of sea level rise [*Clark et al.*, 2007], consistent with IRD peaks in the data occurring after benthic $\delta^{18}O$ begins to decrease (Figure 2). In this respect, the age model for LS16 is consistent with the sea level reconstruction of *Grant et al.* [2012] during H5, H5a, and H6 but not H4.

However, regional phase lags during these events are not well constrained (section 5); we assume synchronous responses except for a 750 year lag applied to the deep Pacific and deep Indian stacks. Also, some aspects of these millennial responses, such as their apparent shapes, may be influenced by the regional alignment targets, particularly in regions with low-amplitude variability and/or relatively few high-resolution records [*Stern and Lisiecki*, 2014]. Therefore, millennial-scale responses are best constrained in the deep North Atlantic stack.

During H8 the deep North Atlantic stack changed by 0.47‰ from 87 to 85.5 ka (Figure 2). Thus, deep North Atlantic benthic $\delta^{18}O$ on its speleothem-correlated age model potentially supports the relative sea level rise of 32 m reconstructed for the Red Sea during H8 [*Grant et al*., 2012]. Coral records additionally provide evidence for 37 m of sea level rise between 91 and 85 ka [*Thompson and Goldstein*, 2006]. The rate of change for deep North Atlantic $\delta^{18}O$ during this event is similar to its rate of change during T2 and H1 (18–15.5 ka).

H12 at ~140 ka may also be associated with a sea level rise of ~30 m [*Grant et al*., 2012; *Rohling et al*., 2014]. Here we discuss the potential role of H12 with respect to the start of T2. *Marino et al*. [2015] refer to this event as MWP-2a and describe it as analogous to the 19 ka meltwater pulse that initiated T1 [*Carlson and Clark*, 2012]; however, H12 occurred during an insolation minimum, whereas the 19 ka event occurred several kiloyears after NHSI began increasing (Figure 4). We suggest that mechanistically H12 is most similar to H3–H5, which were associated with large ice volume, steady or decreasing insolation, and sea level changes of 10–30 m [*Rohling et al*., 2009, 2014]. Our interpretation of H12 as distinct from T2 (and thus unlike the 19 ka meltwater pulse) is supported by a 3–4 kyr hiatus between H12 IRD and the start of T2 as identified by sustained sea level rise, H11 IRD, Antarctic warming, monsoon weakening, and benthic and planktonic $\delta^{18}O$ changes (Figure 4) [*Carlson and Winsor*, 2012; *Govin et al*., 2015]. Therefore, H12 is most similar to H2 with regards to its timing several kiloyears before other indicators of termination onset.

However, H12 appears to be associated with a much larger sea level change than either the 19 ka meltwater pulse or H2 (Figure 4b) [*Clark et al*., 2009]. Thus, H12 may have preconditioned T2 for a fast response to rising insolation by creating smaller, partially deglaciated ice sheets. H12 ice rafting may also explain why some T2 reconstructions show a sea level reversal or an initial rise that precedes insolation change [*Siddall et al*., 2006; *Thomas et al*., 2009; *Medina-Elizalde*, 2013]. Although two high-resolution records suggest a large and rapid rise in relative sea level during H12 [*Grant et al*., 2012; *Rohling et al*., 2014], only very minor responses are observed in many climate records including benthic $\delta^{18}O$ (Figure 4). The climate system may have responded only weakly to ice rafting during H12 due to the background influences of large ice sheets, low insolation, and low CO_2. Benthic $\delta^{18}O$ might also fail to record H12 sea level rise if it was accompanied by deepwater cooling.

Because benthic $\delta^{18}O$ does not respond to this event, our estimated sea level rise by 135 ka at the start of T2 does not include any sea level change associated with H12. We argue that sea level change during H12 is not part of T2 as it lacks many other characteristics of a glacial termination. Thus, the sea level estimate of −85 m at ~137 ka [*Thomas et al*., 2009] could be explained by ~30 m of sea level rise associated with H12 at 140 ka [*Rohling et al*., 2009, 2014] and 10–20 m associated with the beginning of deglaciation from 138 to 135 ka [e.g., *Govin et al*., 2015].

9. Comparison of Terminations 1 and 2

Terminations 1 and 2 display the same basic sequence of events but at a very different pace and with different millennial-scale variability. In both terminations, some ice sheet retreat occurred soon after the first increase in NHSI insolation and before the beginning of global mean benthic $\delta^{18}O$ change [*Carlson and Winsor*, 2012; *Ullman et al*., 2015]. The first rapid benthic $\delta^{18}O$ changes at 135 ka during T2 and at 17.5 ka during T1 appear to correspond to the initiation of similar large-scale global feedback. For both terminations these benthic $\delta^{18}O$ changes are synchronous within error with the start of a large pulse of North Atlantic IRD, WMIs, deglacial CO_2 increase, Greenland stadials, and Southern Hemisphere (SH) warming (Figure 4). A meltwater-induced reduction of AMOC at these times likely triggered bipolar temperature responses and atmospheric shifts that caused weaker monsoons and CO_2 release from the deep ocean [e.g., *Cheng et al*., 2009; *Carlson and Winsor*, 2012]. The bipolar seesaw and associated SH warming may also explain the early $\delta^{18}O$ response observed in the intermediate South Atlantic during both terminations (Figure 4c).

However, meltwater flux from ice sheets must have been greater during H11 (136–129 ka) than H1 (19.5–15 ka); sea level rose by ~30 m over 4.5 kyr during H1 [*Clark et al*., 2009; *Lambeck et al*., 2014] compared to 70 m in 5 kyr during H11 [*Grant et al*., 2012; *Marino et al*., 2015]. The higher melting rate during T2 was likely driven by stronger insolation forcing that weakened AMOC more consistently throughout the termination [*Ruddiman et al*., 1980; *Oppo et al*., 1997; *Carlson*, 2008; *Carlson and Winsor*, 2012], creating continually cold North Atlantic SST and warm SH SST (Figure 4e) [*Govin et al*., 2009; *Hodell et al*., 2009; *Sanchez-Goni et al*., 2012]. Additionally, ice-calving sites or surface currents may have differed because H11 IRD peaks are larger than H1 peaks at high-latitude sites but smaller at middle-latitude sites (Figure S2).

The middles of both terminations are marked by rapid sea level rise as well as plateaus in North Atlantic planktonic $\delta^{18}O$ and Pacific benthic $\delta^{18}O$ (Figure 4). In T1 these features occur during the Bølling-Allerød, accompanied by major North Atlantic warming, relatively little IRD, a plateau in Atlantic benthic $\delta^{18}O$, and an extended interval of strong monsoons. In contrast, millennial-scale climate variability was much weaker during T2; monsoons strengthened only briefly at 134 and 130.5 ka [*Cheng et al*., 2009], deep North Atlantic benthic $\delta^{18}O$ decreased steadily, and IRD continued throughout. Atmospheric pCO_2 [*Landais et al*., 2013; *Marcott et al*., 2014] and South Pacific planktonic $\delta^{18}O$ [*Pahnke et al*., 2003] also change steadily during most of T2 in contrast to step-like changes with minor reversals during T1 (Figure 4). The presence of a deep Pacific benthic $\delta^{18}O$ plateau during T2 despite reduced millennial-scale variability suggests that this plateau may be an inherent feature of terminations caused by meltwater-induced slowing of deep ocean circulation.

Increases in Antarctic temperature and atmospheric pCO_2 had similar durations (6–7 kyr) during both terminations, perhaps because T2 had a greater response amplitude, whereas T1 had more millennial-scale variability [*Röthlisberger et al*., 2008; *Masson-Delmotte et al*., 2010; *Lourantou et al*., 2010; *Marcott et al*., 2014; *Landais et al*., 2013]. In contrast, sea level reconstructions and benthic $\delta^{18}O$ stratigraphy (section 8.1) suggest that ice sheet retreat took 12 kyr during T1 (19–7 ka) compared to only 8 kyr during T2 (136–128 ka). In the 4 kyr after CO_2 and NHSI peaked at 11 ka, sea level rose an additional 54 m [*Clark et al*., 2009; *Carlson and Winsor*, 2012] and benthic $\delta^{18}O$ decreased by 0.34‰. In comparison, T2 sea level and benthic $\delta^{18}O$ reached interglacial levels synchronously with peaks in NHSI and CO_2 at ~128 ka (Figure 4) [*Grant et al*., 2012; *Dutton et al*., 2015]. In summary, faster ice sheet response during T2 likely resulted from stronger insolation forcing, the lack of a midtermination climate reversal, and a potentially large ice-rafting event at 140 ka.

10. Conclusions

New age models for benthic $\delta^{18}O$ are developed by aligning North Atlantic SST and IRD with layer-counted Greenland ice core records and well-dated millennial variability in speleothems. We allow for asynchronous regional $\delta^{18}O$ change during T1 and T2 and apply a constant 750 year lag to the deep Pacific and deep Indian regions. Regional phase lags are not well constrained but are likely less than 2 kyr except during terminations. We use Monte Carlo-style sampling to estimate the potential effects of different regional lags. Improved estimates could likely be derived from modeling experiments.

Age estimates for many marine sediment cores that lack other means of dating (e.g., radiocarbon or correlation with nearby terrestrial records) would likely be improved by alignment to the regional benthic $\delta^{18}O$ stacks, which provide better alignment targets than a global stack. For example, the MIS 5e/5d transition and MIS 5c appear to exhibit significant regional variability.

We also develop a volume-weighted LS16 global $\delta^{18}O$ stack to compare with the LR04 global stack [*Lisiecki and Raymo*, 2005] and estimates of sea level change. The new global stack matches the timing of sea level reconstructions for T1 and T2 [*Clark et al*., 2009; *Lambeck et al*., 2014; *Grant et al*., 2012] to within ~1000 years and is 1–4 kyr older than LR04 during T2, MIS 5e-5d, MIS 4, and the first half of MIS 3. Collectively, these age model differences suggest that the response time used for tuning the Pleistocene portion of LR04 was too large. We estimate new parameter values for $\delta^{18}O$ tuning targets that better fit the LS16 stack and would shift the LR04 stack older by 1–2 kyr from 0.15 to 1.5 Ma.

Heinrich events during MIS 3 and 5 are associated with $\delta^{18}O$ decreases of 0.2–0.4‰ in all regions, but these features may be biased by our alignment targets. However, $\delta^{18}O$ change during H8 in the deep North Atlantic is well constrained by correlation to speleothems and indicates a rapid $\delta^{18}O$ response similar to H1 and H11, thus potentially supporting estimates that relative sea level rose 32 m in ~2 kyr [*Grant et al*., 2012].

Two high-resolution records suggest a rapid rise in relative sea level of ~30 m during H12 [*Grant et al*., 2012; *Rohling et al*., 2014] at 140 ka, 3–4 kyr before the start of T2. Subsequently, rising NHSI beginning at 139 ka triggered the start of deglaciation, which produced another 9–17 m of sea level rise by 135 ± 2.5 ka, as estimated from global and regional benthic $\delta^{18}O$ changes. Together, these two sea level rise events may explain a sea level height of −85 m at ~137 ka [*Thomas et al*., 2009]. We argue that ice sheets responded to insolation more quickly during T2 than T1 due to both stronger insolation forcing [*Ruddiman et al*., 1980; *Carlson*, 2008; *Marino et al*., 2015] and the pretermination ice-rafting event. Thus, differences in insolation forcing and millennial variability during the two terminations explain why deglaciation took 12 kyr during T1 (19–7 ka) compared to only 8 kyr during T2 (136–128 ka).

Appendix A: Data Sources

Data from the following sources were used to create the benthic $\delta^{18}O$ stacks. See Table S1 for more details [*Ahmad et al*., 2008; *Andreasen et al*., 2000; *Arz et al*., 1999; *Baas et al*., 1997; *Bard et al*., 1989, 1994, 2004; *Becquey and Gersonde*, 2003; *Behling et al*., 2002; *Bickert et al*., 1993, 1997; *Bickert and Wefer*, 1996; *Black et al*., 1988; *Bond et al*., 1997; *Boyle and Keigwin*, 1985; *Broecker*, 1988; *Came et al*., 2003, 2007; *Channell et al*., 1997; *Chapman and Shackleton*, 1998, 1999; *Charles and Fairbanks*, 1992; *Charles et al*., 1991, 1996; *Chen and Huang*, 1998; *Chen et al*., 1995; *Cheng et al*., 2004; *Clemens and Prell*, 2003; *Clemens et al*., 2008; *Collins et al*., 2011; *Cortijo*, 1995; *Cortijo et al*., 1999; *Curry et al*., 1988, 1999; *Curry and Lohmann*, 1983; *Curry and Oppo*, 1997, 2005; *de Abreu et al*., 2003; *deMenocal et al*., 2000; *Dickson et al*., 2008, 2009; *Dudley and Nelson*, 1994; *Duplessy*, 1982, 1996; *Duplessy et al*., 1988, 1992, 2007; *Durkop et al*., 2008; *Elliot et al*., 1998, 2002; *Eynaud et al*., 2007; *Freudenthal et al*., 2002; *Ganeshram and Pedersen*, 1998; *Gardner et al*., 1997; *Gebhardt et al*., 2008; *Gherardi et al*., 2005; *Grousset et al*., 1993; *Hagen and Keigwin*, 2002; *Hall et al*., 2001; *Hendy and Kennett*, 2000; *Herbert et al*., 2001; *Heusser and Oppo*, 2003; *Hillenbrand et al*., 2002; *Hodell et al*., 2000, 2003, 2008, 2009; *Holbourn et al*., 2005; *Hoogakker et al*., 2007, 2011; *Hovan et al*., 1991; *Hüls*, 2000; *Hüls and Zahn*, 2000; *Imbrie et al*., 1989; *Isono et al*., 2009; *Jansen and Veum*, 1990; *Jullien et al*., 2006; *Jung*, 1996; *Keigwin and Jones*, 1989, 1994; *Keigwin et al*., 1991, 1994; *Keigwin*, 1995; *Labeyrie et al*., 1995, 1996, 1999; *Labracherie et al*., 1989; *Lackschewitz et al*., 1998; *Lalicata and Lea*, 2011; *Lea et al*., 2002, 2006; *Lebreiro et al*., 2009; *Lee et al*., 1999; *Lisiecki et al*., 2008; *Little et al*., 1997; *Loubere et al*., 2003; *Lyle et al*., 1992, 2000, 2002; *Mackensen and Bickert*, 1999; *Mackensen et al*., 1994, 2001; *Marchitto et al*., 2005; *Martin et al*., 2002; *Martinson et al*., 1987; *McIntyre et al*., 1989; *McManus et al*., 1999; *Millo et al*., 2006; *Mix*, 1986; *Mix and Fairbanks*, 1985; *Mix et al*., 1991, 1995a, 1995b; *Mohtadi et al*., 2006; *Mojtahid et al*., 2005; *Molyneux et al*., 2007; *Mortyn et al*., 1996; *Mulitza et al*., 2008; *Murray et al*., 2000; *Nelson et al*., 1986, 1993; *Ninkovitch and Shackleton*, 1975; *Nürnberg et al*., 2004; *Oba and Murayama*, 2004; *Oba et al*., 2006; *Ohkushi et al*., 2003; *Oppo et al*., 1990, 1997, 2001; *Oppo and Fairbanks*, 1987, 1990; *Oppo and Horowitz*, 2000; *Oppo and Lehman*, 1995; *Oppo and Sun*, 2005; *Ostermann and Curry*, 2000; *Pahnke et al*., 2003; *Pahnke and Zahn*, 2005; *Pierre et al*., 2001; *Pichevin et al*., 2005; *Pichon et al*., 1992; *Piotrowski et al*., 2004; *Pisias and Mix*, 1997; *Praetorius et al*., 2008; *Raymo et al*., 1997, 2004; *Richter*, 1998; *Ruddiman and McIntyre*, 1981; *Rühlemann et al*., 1999, 2004; *Russon et al*., 2009; *Saikku et al*., 2009; *Salgueiro et al*., 2010; *Samson et al*., 2005; *Sanchez-Goni et al*., 2005; *Sarnthein et al*., 1994, 2004, 2005, 2007; *Schlünz et al*., 2000; *Schmiedl and Mackensen*, 1997, 2006; *Schönfeld et al*., 2003; *Shackleton*, 1977; *Shackleton et al*., 1983, 1990, 2000, 2004; *Shackleton and Hall*, 1989; *Sikes et al*., 2009; *Sirocko et al*., 1993, 2000; *Skinner et al*., 2003, 2010; *Skinner and Shackleton*, 2004, 2005; *Slowey and Curry*, 1995; *Smart et al*., 2010; *Sowers et al*., 1993; *Stott*, 2007; *Stott et al*., 2000, 2007; *Thornalley et al*., 2010; *Tian et al*., 2002; *Tiedemann et al*., 1994; *Tjallingii et al*., 2008; *Toucanne et al*., 2009; *van Kreveld et al*., 2000; *Vautravers et al*., 2004; *Venz et al*., 1999; *Vidal et al*., 1999; *Voelker et al*., 2006; *Waddell et al*., 2009; *Waelbroeck et al*., 2001, 2011; *Wang et al*., 1999; *Weaver et al*., 1998; *Wei et al*., 2006; *Weinelt*, 1993; *Weinelt et al*., 2003; *Wells and Okada*, 1997; *Winn et al*., 1991; *Yamane*, 2003; *Zabel et al*., 1999; *Zahn et al*., 1986; *Zarriess and Mackensen*, 2010, 2011; *Zarriess et al*., 2011; *Zhang et al*., 2007].

Acknowledgments

All data are archived in the supporting information and at the World Data Center for Paleoclimatology operated by the National Climatic Data Center of the National Oceanographic and Atmospheric Association (https://www.ncdc.noaa.gov/paleo/study/20486). Support is provided by the National Science Foundation grant MGG-0926735. We also thank all researchers who made their $\delta^{18}O$ data available, S. Barker for providing his revised SpeleoAge chronology, L. Skinner A. Carlson, anonymous reviewers for their helpful critiques, and A. Jones for the formatting assistance.

References

Abe-Ouchi, A., F. Saito, K. Kawamura, M. E. Raymo, J. Okuno, K. Takahashi, and H. Blatter (2013), Insolation-driven 100,000-year glacial cycles and hysteresis of ice-sheet volume, *Nature*, *500*, 190–193, doi:10.1038/nature12374.

Adkins, J. F., K. McIntyre, and D. P. Schrag (2002), The salinity, temperature, and $\delta^{18}O$ of the glacial deep ocean, *Science*, *298*, 1769–1773.

Ahmad, S. M., G. A. Babu, V. M. Padmakumari, and W. Raza (2008), Surface and deep water changes in the northeast Indian Ocean during the last 60 ka inferred from carbon and oxygen isotopes of planktonic and benthic foraminifera, *Palaeogeogr. Palaeoclimatol. Palaeoecol.*, *262*(3-4), 182–188, doi:10.1016/j.paleo.2008.03.007.

Ahn, J., and E. J. Brook (2008), Atmospheric CO_2 and climate on millennial time scales during the last glacial period, *Science*, *322*, 83–85, doi:10.1126/science.1160832.

Andreasen, D. H., M. Flower, M. Harvey, S. Chang, and A. C. Ravelo (2000), Late Pleistocene oxygen and carbon isotopic records from Sites 1011, 1012, and 1018, in *Proceedings of the Ocean Drilling Program*, *Sci. Results*, vol. 167, edited by M. Lyle et al., pp. 141–144, Ocean Drilling Program, College Station, Tex.

Arz, H. W., J. Patzold, and G. Wefer (1999), The deglacial history of the western tropical Atlantic as inferred from high resolution stable isotope records off northeastern Brazil, *Earth Planet. Sci. Lett.*, *167*, 105–117, doi:10.1016/S0012-821X(99)00025-4.

Baas, J. H., J. Mienert, F. Abrantes, and M. A. Prins (1997), Late Quaternary sedimentation on the Portuguese continental margin: Climate-related processes and products, *Palaeogeogr. Palaeoclimatol. Palaeoecol.*, *130*, 1–23.

Bard, E., R. Fairbanks, M. Arnold, P. Maurice, J. Duprat, J. Moyes, and J.-C. Duplessy (1989), Sea-level estimates during the last deglaciation based on $\delta^{18}O$ and accelerator mass spectrometry ^{14}C ages measured in *Globigerina bulloides*, *Quat. Res.*, *31*, 381–391.

Bard, E., B. Hamelin, and R. G. Fairbanks (1990), U-Th ages obtained by mass spectrometry in corals from Barbados: Sea-level during the past 130,000 years, *Nature*, *346*, 456–458, doi:10.1038/346456a0.

Bard, E., M. Arnold, J. Mangerud, M. Paterne, L. Labeyrie, J. Duprat, M.-A. Mélières, E. Søntstegaard, and J.-C. Duplessy (1994), The North Atlantic atmosphere-sea surface ^{14}C gradient during the Younger Dryas climatic event, *Earth Planet. Sci. Lett.*, *126*(4), 275–287, doi:10.1016/0012-821X(94)90112-0.

Bard, E., F. Rostek, and G. Ménot-Combes (2004), Radiocarbon calibration beyond 20,000 ^{14}C yr B.P. by means of planktonic foraminifera of the Iberian Margin, *Quat. Res.*, *61*(2), 204–214, doi:10.1016/j.yqres.2003.11.006.

Barker, S., and P. Diz (2014), Timing of the descent into the Last Ice Age determined by the bipolar seesaw, *Paleoceanography*, *29*, 489–507, doi:10.1002/2014PA002623.

Barker, S., G. Knorr, R. Edwards, F. Parrenin, A. Putnam, L. Skinner, E. Wolff, and M. Ziegler (2011), 800,000 years of abrupt climate variability, *Science*, *334*, 347–351, doi:10.1126/science.1203580.

Bazin, L., et al. (2013), An optimized multi-proxy, multi-site Antarctic ice and gas orbital chronology (AICC2012): 120–800 ka, *Clim. Past*, *9*, 1715–1731, doi:10.5194/cp-9-1715-2013.

Becquey, S., and R. Gersonde (2003), A 0.55-Ma paleotemperature record from the Subantarctic zone: Implications for Antarctic Circumpolar Current development, *Paleoceanography*, *18*(1), 1014, doi:10.1029/2000PA000576.

Behling, H., H. W. Arz, J. Patzold, and G. Wefer (2002), Late Quaternary vegetational and climate dynamics in southeastern Brazil, inferences from marine cores GeoB 3229-2 and GeoB 3202-1, *Palaeogeogr. Palaeoclimatol. Palaeoecol.*, *179*, 227–243.

Bickert, T., and G. Wefer (1996), Late Quaternary deep water circulation in the South Atlantic: Reconstruction from carbonate dissolution and benthic stable isotopes, in *The South Atlantic: Present and Past Circulation*, edited by G. Wefer et al., pp. 599–620, Springer, New York.

Bickert, T., W. H. Berger, S. Burke, H. Schmidt, and G. Wefer (1993), Late Quaternary stable isotope record of benthic foraminifers: Site 805 and 806, Ontong Java Plateau, in *Proceedings of the Ocean Drilling Program*, *Sci. Results*, vol. 130, edited by W. H. Berger et al., pp. 411–420, Ocean Drilling Program, College Station, Tex., doi:10.2973/odp.proc.sr.130.025.1993.

Bickert, T., W. B. Curry, and G. Wefer (1997), Late Pliocene to Holocene (2.6–0 Ma) western equatorial Atlantic deep-water circulation: Inferences from benthic stable isotopes, in *Proceedings of the Ocean Drilling Program*, *Sci. Results*, vol. 154, edited by N. J. Shackleton et al., pp. 239–254, Ocean Drilling Program, College Station, Tex.

Bintanja, R., R. S. W. van de Wal, and J. Oerlemans (2005), Modelled atmospheric temperatures and global sea levels over the past million years, *Nature*, *437*, 125–128, doi:10.1038/nature03975.

Blaauw, M., and J. A. Christen (2011), Flexible paleoclimate age-depth models using an autoregressive gamma process, *Bayesian Anal.*, *6*, 457–474, doi:10.5194/cp-9-1715-2013.

Black, K. P., C. S. Nelson, and C. H. Hendy (1988), A spectral analysis procedure for dating Quaternary deep-sea cores and its application to a high-resolution Brunhes record from the Southwest Pacific, *Mar. Geol.*, *83*, 21–30.

Boch, R., H. Cheng, C. Spoetl, R. L. Edwards, X. Wang, and P. Haeuselmann (2011), NALPS: A precisely dated European climate record 120–60 ka, *Clim. Past*, *7*(4), 1247–1259, doi:10.5194/cp-7-1247-2011.

Böhm, E., J. Lippold, M. Gutjahr, M. Frank, P. Blaser, B. Antz, J. Fohlmeister, N. Frank, M. B. Andersen, and M. Deininger (2015), Strong and deep Atlantic meridional overturning circulation during the last glacial cycle, *Nature*, *517*, 73–76, doi:10.1038/nature14059.

Bond, G., W. Showers, M. Cheseby, R. Latti, P. Almasi, P. deMenocal, P. Priore, H. Cullen, I. Hajdas, and G. Bonani (1997), A pervasive millennial-scale cycle in North Atlantic Holocene and glacial climates, *Science*, *278*, 1257–1266.

Boyle, E. A., and L. D. Keigwin (1985), Comparison of Atlantic and Pacific paleochemical records for the last 215,000 years: Changes in deep ocean circulation and chemical inventories, *Earth Planet. Sci. Lett.*, *76*, 135–150.

Broecker, W. S. (1988), Paleocean circulation during the last deglaciation: A bipolar seesaw?, *Paleoceanography*, *13*(2), 119–121, doi:10.1029/97PA03707.

Broecker, W. S., D. Oppo, T. Peng, W. Curry, M. Andree, W. Wolfli, and G. Bonani (1988), Radiocarbon-based chronology for the $^{18}O/^{16}O$ record for the last deglaciation, *Paleoceanography*, *3*(4), 509–515, doi:10.1029/PA003i004p00509.

Bühring, C., M. Sarnthein, and Leg 184 Shipboard Scientific Party (2000), Toba ash layers in the South China Sea: Evidence of contrasting wind directions during eruption ca. 74 ka, *Geology*, *28*, 275–278, doi:10.1130/0091-7613.

Caballero-Gill, R. P., S. C. Clemens, and W. L. Prell (2012), Direct correlation of Chinese speleothem $\delta^{18}O$ and South China Sea planktonic $\delta^{18}O$: Transferring a speleothem chronology to the benthic marine chronology, *Paleoceanography*, *27*, PA2203, doi:10.1029/2011PA002268.

Came, R. E., D. W. Oppo, and W. B. Curry (2003), Atlantic Ocean circulation during the Younger Dryas: Insights from a new Cd/Ca record from the western subtropical South Atlantic, *Paleoceanography*, *18*(4), 1086, doi:10.1029/2003PA000888.

Came, R. E., D. W. Oppo, and J. F. McManus (2007), Amplitude and timing of salinity and temperature variability in the high-latitude North Atlantic, *Geology*, *35*, 315–318.

Carlson, A. E. (2008), Why there was not a Younger Dryas-like event during the penultimate deglaciation, *Quat. Sci. Rev.*, *27*, 882–887.

Carlson, A. E., and K. Winsor (2012), Northern Hemisphere ice-sheet responses to past climate warming, *Nat. Geosci.*, *5*, 607–613, doi:10.1038/NGEO1528.

Carlson, A. E., and P. U. Clark (2012), Ice sheet sources of sea level rise and freshwater discharge during the last deglaciation, *Rev. Geophys.*, *50*, RG4007, doi:10.1029/2011RG000371.

Channell, J. E. T., D. A. Hodell, and B. Lehman (1997), Relative geomagnetic paleointensity and $\delta^{18}O$ at ODP Site 983 (Gardar Drift, North Atlantic) since 350 ka, *Earth Planet. Sci. Lett.*, *153*, 103–118.

Channell, J. E. T., D. A. Hodell, O. Romero, C. Hillaire-Marcel, A. de Vernal, J. S. Stonere, A. Mazaud, and U. Röhl (2012), A 750-kyr detrital-layer stratigraphy for the North Atlantic (IODP Sites U1302-U1303, Orphan Knoll, Labrador Sea), *Earth Planet. Sci. Lett.*, *317-318*, 218–230, doi:10.1016/j.epsl.2011.11.029.

Chapman, M. R., and N. J. Shackleton (1998), Millennial-scale fluctuations in North Atlantic heat flux during the last 150,000 years, *Earth Planet. Sci. Lett.*, *159*(1), 57–70, doi:10.1016/S0012-821X(98)00068-5.

Chapman, M. R., and N. J. Shackleton (1999), Global ice-volume fluctuations, North Atlantic ice-rafting events, and deep-ocean circulation changes between 130 and 70 ka, *Geology*, *27*, 795–798, doi:10.1130/0091-7613(1999)027.

Charles, C. D., and R. G. Fairbanks (1992), Evidence from Southern Ocean sediments for the effect of North Atlantic deep-water flux on climate, *Nature*, *355*, 416–419.

Charles, C. D., P. N. Froelich, M. A. Zibello, R. A. Mortlock, and J. J. Morley (1991), Biogenic opal in southern ocean sediments over the last 450,000 years: Implications for surface water chemistry and circulation, *Paleoceanography*, *6*, 697–728, doi:10.1029/91PA02477.

Charles, C. D., J. Lynch-Stieglitz, U. S. Ninnemann, and R. G. Fairbanks (1996), Climate connections between the hemisphere revealed by deep sea sediment core/ice core correlations, *Earth Planet. Sci. Lett.*, *142*, 19–27.

Chen, J. H., H. A. Curran, B. White, and G. J. Wasserburg (1991), Precise chronology of the last interglacial period: ^{234}U-^{230}Th data from fossil coral reefs in the Bahamas, *GSA Bull.*, *103*(1), 82–97, doi:10.1130/0016-7606.

Chen, J., J. W. Farrell, D. Murray, and W. L. Prell (1995), Timescale and paleoceanographic implications of a 3.6 m.y. oxygen isotope record from the northeast Indian Ocean (Ocean Drilling Program Site 758), *Paleoceanography*, *10*, 21–48, doi:10.1029/94PA02290.

Chen, M., and C. Huang (1998), Ice-volume forcing of winter monsoon climate in the South China Sea, *Paleoceanography*, *13*(6), 622–633, doi:10.1029/98PA02356.

Cheng, H., R. L. Edwards, Y. Wang, X. Kong, Y. Ming, M. J. Kelly, X. Wang, C. D. Gallup, and W. Liu (2006), A penultimate glacial monsoon record from Hulu Cave and two-phase glacial terminations, *Geology*, *34*, 217–220, doi:10.1130/G22289.1.

Cheng, H., R. Edwards, W. Broecker, G. Denton, X. Kong, Y. Wang, R. Zhang, and X. Wang (2009), Ice age terminations, *Science*, *326*, 248–252, doi:10.1126/science.1177840.

Cheng, X., J. Tian, and P. Wang (2004), Stable isotopes from Site 1143, in *Proceedings of the Ocean Drilling Program*, *Sci. Results*, vol. 184, edited by W. L. Prellpp et al., pp. 1–8, Ocean Drilling Program, College Station, Tex.

Clark, P. U., S. W. Hostetler, N. G. Pisias, A. Schmittner, and K. J. Meissner (2007), Mechanisms for an ~7-kyr climate and sea-level oscillation during marine isotope stage 3, in *Ocean Circulation: Mechanisms and Impacts*, *Geophys. Monogr. Ser.*, vol. 173, pp. 209–246, AGU, Washington, D. C., doi:10.1029/173GM15.

Clark, P. U., A. Dyke, J. Shakun, A. Carlson, J. Clark, B. Wohlfarth, J. Mitrovica, S. Hostetler, and A. McCabe (2009), The Last Glacial Maximum, *Science*, *325*(5941), 710–714, doi:10.1126/science.1172873.

Clemens, S. C., and W. L. Prell (2003), Oxygen and carbon isotopes from Site 1146, northern South China Sea, in *Proceedings of the Ocean Drilling Program*, *Sci. Results*, vol. 184, edited by W. L. Prell et al., pp. 1–8, Ocean Drilling Program, College Station, Tex., doi:10.2973/odp.proc.sr.184.214.2003.

Clemens, S. C., W. L. Prell, Y. Sun, Z. Liu, and G. Chen (2008), Southern Hemisphere forcing of Pliocene δ^{18}O and the evolution of Indo-Asian monsoons, *Paleoceanography*, *23*, PA4210, doi:10.1029/2008PA001638.

Collins, J. A., et al. (2011), Interhemispheric symmetry of the tropical African rainbelt over the past 23,000 years, *Nat. Geosci.*, *4*(1), 42–45, doi:10.1038/ngeo1039.

Cortijo, E. (1995), La variabilité climatique rapide dans l'Atlantique Nord depuis 128,000 ans: Relations entre les calottes de glace et l'océan de surface PhD thesis, Univ. de Paris-Sud, Paris, France.

Cortijo, E., S. Lehman, L. Keigwin, M. Chapman, D. Paillard, and L. Labeyrie (1999), Changes in meridional temperature and salinity gradients in the North Atlantic Ocean (30°-72°N) during the last interglacial period, *Paleoceanography*, *14*(1), 22–33, doi:10.1029/1998PA900004.

Coyne, M. K., B. Jones, and D. Ford (2007), Highstands during marine isotope stage 5: Evidence from the Ironshore Formation of Grand Cayman, British West Indies, *Quat. Sci. Rev.*, *26*, 536–559, doi:10.1016/j.quascirev.2006.06.013.

Curry, W. B., and D. W. Oppo (1997), Synchronous, high-frequency oscillations in tropical sea surface temperatures and North Atlantic Deep Water productivity during the last glacial cycle, *Paleoceanography*, *12*(1), 1–14, doi:10.1029/96PA02413.

Curry, W. B., and D. W. Oppo (2005), Glacial water mass geometry and the distribution of δ^{13}C of ΣCO_2 in the western Atlantic Ocean, *Paleoceanography*, *20*, PA1017, doi:10.1029/2004PA001021.

Curry, W. B., and G. P. Lohmann (1983), Reduced advection into Atlantic Ocean deep eastern basins during last glaciation maximum, *Nature*, *306*, 577–580, doi:10.1038/306577a0.

Curry, W. B., J.-C. Duplessy, L. D. Labeyrie, and N. J. Shackleton (1988), Changes in the distribution of δ^{13}C of deep water ΣCO_2 between the last glaciation and the Holocene, *Paleoceanography*, *3*, 317–341, doi:10.1029/PA003i003p00317.

Curry, W. B., T. M. Marchitto, J. F. McManus, D. W. Oppo, and K. L. Laarkamp (1999), Millennial-scale changes in ventilation of the thermocline, intermediate, and deep waters of the glacial North Atlantic, *Geophys. Monogr. Ser.*, *112*, 59–76.

De Abreu, L., N. J. Shackleton, J. Schönfeld, M. Hall, and M. Chapman (2003), Millennial-scale oceanic climate variability off the Western Iberian margin during the last two glacial periods, *Mar. Geol.*, *196*(1-2), 1–20, doi:10.1016/S0025-3227(03)00046-X.

deMenocal, P., J. Ortiz, T. Guilderson, J. Adkins, M. Sarnthein, L. Baker, and M. Yarusinsky (2000), Abrupt onset and termination of the African Humid Period: Rapid climate responses to gradual insolation forcing, *Quat. Sci. Rev.*, *19*(1), 347–361, doi:10.1016/S0277-3791(99)00081-5.

Dickson, A. J., W. E. N. Austin, I. R. Hall, M. A. Maslin, and M. Kucera (2008), Centennial-scale evolution of Dansgaard-Oeschger events in the northeast Atlantic Ocean between 39.5 and 56.5 ka B.P, *Paleoceanography*, *23*, PA3206, doi:10.1029/2008PA001595.

Dickson, A. J., C. J. Beer, C. Dempsey, M. A. Maslin, J. A. Bendle, E. L. McClymont, and R. D. Pancost (2009), Oceanic forcing of the marine isotope stage 11 interglacial, *Nat. Geosci.*, *2*, 428–433.

Dong, J., et al. (2010), A high-resolution stalagmite record of the Holocene East Asian monsoon from Mt. Shennongjia, central China, *Holocene*, *20*(2), 257–264, doi:10.1177/O959683609350393.

Drysdale, R. N., J. Hellstrom, G. Zanchetta, A. E. Fallick, M. F. Sánchez Goñi, I. Couchoud, J. McDonald, R. Maas, G. Lohmann, and I. Isola (2009), Evidence for obliquity forcing of glacial Termination II, *Science*, *325*, 1527–1531, doi:10.1126/science.1170371.

Dudley, W. C., and C. S. Nelson (1994), The influence of non-equilibrium isotope fractionation on the Quaternary calcareous nanofossil stable isotope signal in the southwest Pacific Ocean, DSDP Site 594, *Mar. Micropaleontol.*, *24*, 3–27.

Duplessy, J.-C. (1982), North Atlantic Deep Water circulation during the last climate cycle, *Bull. Inst. Geol. Bassin Aquitaine*, *31*, 379–391.

Duplessy, J.-C. (1996), Quaternary paleoceanography: Unpublished stable isotope records IGBP PAGES/World Data Center for Paleoclimatology Data Contribution Series #1996-035, NOAA/NGDC Paleoclimatology Program, Boulder, Colo.

Duplessy, J.-C., N. J. Shackleton, R. G. Fairbanks, L. Labeyrie, D. Oppo, and N. Kallel (1988), Deepwater source variations during the last climatic cycle and their impact on the global deepwater circulation, *Paleoceanography*, *3*(3), 343–360, doi:10.1029/PA003i003p00343.

Duplessy, J.-C., L. Labeyrie, M. Arnold, M. Paterne, J. Duprat, and T. C. E. van Weering (1992), Changes in surface salinity of the North Atlantic Ocean during the last deglaciation, *Nature*, *358*(6386), 485–488, doi:10.1038/358485a0.

Duplessy, J.-C., L. Labeyrie, and C. Waelbroeck (2002), Constraints on the ocean oxygen isotopic enrichment between the Last Glacial Maximum and the Holocene: Paleoceanographic implications, *Quat. Sci. Rev.*, *21*, 315–330, doi:10.1016/S0277-3791(01)00107-X.

Duplessy, J.-C., D. M. Roche, and M. Kageyama (2007), The deep ocean during the last interglacial period, *Science*, *316*, 89–91.

Durkop, A., A. E. L. Holbourn, W. Kuhnt, R. Zuraida, N. Andersen, and P. M. Grootes (2008), Centennial-scale climate variability in the Timor Sea during marine isotope stage 3, *Mar. Micropaleontol.*, *66*, 208–221, doi:10.1016/j.marmicro.2007.10.002.

Dutton, A., J. M. Webster, D. Zwartz, K. Lambeck, and B. Wohlfarth (2015), Tropical tales of polar ice: Evidence of last interglacial polar ice sheet retreat recorded by fossil reefs of the granitic Seychelles islands, *Quat. Sci. Rev.*, *107*, 182–196, doi:10.1016/j.quascirev.2014.10.025.

Elderfield, H., M. Greaves, S. Barker, I. R. Hall, A. Tripati, P. Ferretti, S. Crowhurst, L. Booth, and C. Daunt (2010), A record of bottom water temperature and seawater $\delta^{18}O$ for the Southern Ocean over the past 440 kyr based on Mg/Ca of benthic foraminiferal *Uvigerina* spp, *Quat. Sci. Rev.*, *29*, 160–169.

Elderfield, H., P. Ferretti, M. Greaves, S. Crowhurst, I. N. McCave, D. Hodell, and A. M. Piotrowski (2012), Evolution of ocean temperature and ice volume through the Mid-Pleistocene climate transition, *Science*, *337*, 704–709, doi:10.1126/science.1221294.

Elliot, M., L. Labeyrie, G. Bond, E. Cortijo, J.-L. Turon, N. Tisnerat, and J.-C. Duplessy (1998), Millennial-scale iceberg discharges in the Irminger Basin during the last glacial period: Relationship with the Heinrich events and environmental settings, *Paleoceanography*, *13*(5), 433–446, doi:10.1029/98PA01792.

Elliot, M., L. Labeyrie, and J.-C. Duplessy (2002), Changes in North Atlantic deep-water formation associated with the Dansgaard-Oeschger temperature oscillations (60–10 ka), *Quat. Sci. Rev.*, *21*(10), 1153–1165, doi:10.1016/S0277-3791(01)00137-8.

Esat, T. M., M. T. McCulloch, J. Chappell, B. Pillans, and A. Omura (1999), Rapid fluctuations in sea level recorded at Huon Peninsula during the penultimate deglaciation, *Science*, *283*, 197–201, doi:10.1126/science.283.5399.197.

Eynaud, F., S. Zaragosi, J. D. Scourse, M. Mojtahid, J. F. Bourillet, I. R. Hall, A. Penaud, M. Locascio, and A. Reijonen (2007), Deglacial laminated facies on the NW European continental margin: The hydrographic significance of British-Irish Ice Sheet deglaciation and Fleuve Manche paleoriver discharges, *Geochem. Geophys. Geosyst.*, *8*, Q06019, doi:10.1029/2006GC001496.

Freudenthal, T., H. Meggers, J. Henderiks, H. Kuhlmann, A. Moreno, and G. Wefer (2002), Upwelling intensity and filament activity off Morocco during the last 250,000 years, *Deep Sea Res., Part II*, *49*, 3655–3674.

Gallup, C. D., H. Cheng, F. W. Taylor, and R. L. Edwards (2002), Direct determination of the timing of sea level change during Termination II, *Science*, *295*, 310–313, doi:10.1126/science.1065494.

Ganeshram, R. S., and T. F. Pedersen (1998), Glacial-interglacial variability in upwelling and bioproductivity off NW Mexico: Implications for Quaternary paleoclimate, *Paleoceanography*, *13*, 634–645, doi:10.1029/98PA02508.

Garcia-Olivares, A., and C. Herrero (2013), Simulation of glacial-interglacial cycles by simple relaxation models: Consistency with observational results, *Clim. Dyn.*, *41*, 1307–1331, doi:10.1007/s00382-012-1614-7.

Gardner, J. V., W. E. Dean, and P. Dartnell (1997), Biogenic sedimentation beneath the California Current system for the past 30 kyr and its paleoceanographic significance, *Paleoceanography*, *12*(2), 207–225, doi:10.1029/96PA03567.

Gebbie, G. (2012), Tracer transport timescales and the observed Atlantic-Pacific lag in the timing of the Last Termination, *Paleoceanography*, *27*, PA3225, doi:10.1029/2011PA002273.

Gebbie, G., and P. Huybers (2012), The mean age of ocean waters inferred from radiocarbon observations: Sensitivity to surface sources and accounting for mixing histories, *J. Phys. Oceanogr.*, *42*, 291–305, doi:10.1175/JPO-D-11-043.1.

Gebhardt, H., M. Sarnthein, P. M. Grootes, T. Kiefer, H. Kuehn, F. Schmieder, and U. Röhl (2008), Paleonutrient and productivity records from the subarctic North Pacific for Pleistocene glacial terminations I to V, *Paleoceanography*, *23*, PA4212, doi:10.1029/2007PA001513.

Gherardi, J.-M., L. Labeyrie, J. F. McManus, R. Francois, L. C. Skinner, and E. Cortijo (2005), Evidence from the Northeastern Atlantic basin for variability in the rate of the meridional overturning circulation through the last deglaciation, *Earth Planet. Sci. Lett.*, *240*(3-4), 710–723, doi:10.1016/j.epsl.2005.09.061.

Govin, A., E. Michel, L. Labeyrie, C. Waelbroeck, F. Dewilde, and E. Jansen (2009), Evidence for northward expansion of Antarctic bottom water mass in the Southern Ocean during the last glacial inception, *Paleoceanography*, *24*, PA1202, doi:10.1029/2008PA001603.

Govin, A., et al. (2012), Persistent influence of ice sheet melting on high northern latitude climate during the early Last Interglacial, *Clim. Past*, *8*, 483–507, doi:10.5194/cp-8-483-2012.

Govin, A., et al. (2015), Sequence of events from the onset to the demise of the Last Interglacial: Evaluating strengths and limitations of chronologies used in climatic archives, *Quat. Sci. Rev.*, *129*, 1–36.

Grant, K. M., E. J. Rohling, M. Bar-Matthews, A. Ayalon, M. Medina-Elizalde, C. Ramsey, C. Satow, and A. P. Roberts (2012), Rapid coupling between ice volume and polar temperature over the past 150,000 years, *Nature*, *491*, 744–747, doi:10.138/nature11593.

Grousset, F. E., L. Labeyrie, J. A. Sinko, M. Cremer, G. C. Bond, J. Duprat, E. Cortijo, and S. Huon (1993), Patterns of ice-rafted detritus in the glacial North Atlantic (40-55°N), *Paleoceanography*, *8*(2), 175–192, doi:10.1029/92PA02923.

Hagen, S., and L. D. Keigwin (2002), Sea-surface temperature variability and deep water reorganization in the subtropical North Atlantic during isotope stage 2-4, *Mar. Geol.*, *189*, 145–162.

Hall, I. R., I. N. McCave, N. J. Shackleton, G. P. Weedon, and S. E. Harris (2001), Intensified deep Pacific inflow and ventilation in Pleistocene glacial times, *Nature*, *412*, 809–812.

Heinrich, H. (1988), Origin and consequences of cyclic ice rafting in the northeast Atlantic Ocean during the past 130,000 years, *Quat. Res.*, *29*(2), 142–152, doi:10.1016/0033-5894(88)90057-9.

Hendy, I. L., and J. P. Kennett (2000), Stable isotope stratigraphy and paleoceanography of the last 170 k.y.: Site 1014, Tanner Basin, California, in *Proceedings of the Ocean Drilling Program*, *Sci. Results*, vol. 167, edited by M. Lyle et al., pp. 129–140, Ocean Drilling Program, College Station, Tex.

Herbert, T. D., J. D. Schuffert, D. Andreasen, L. Heusser, M. Lyle, A. Mix, A. C. Ravelo, L. D. Stott, and J. C. Herguera (2001), Collapse of the California Current during glacial maxima linked to climate change on land, *Science*, *293*, 71–76.

Heusser, L., and D. W. Oppo (2003), Millennial- and orbital-scale climate variability in southeastern United States and in the subtropical Atlantic during marine isotope stage 5: Evidence from pollen and isotopes in ODP Site 1059, *Earth Planet. Sci. Lett.*, *214*(3–4), 483–490.

Hillenbrand, C. D., D. K. Futterer, H. Grobe, and T. Frederichs (2002), No evidence for a Pleistocene collapse of the West Antarctic Ice Sheet from continental margin sediments recovered in the Amundsen Sea, *Geo-Mar. Lett.*, *22*, 51–59.

Hodell, D. A., C. D. Charles, and U. S. Ninnemann (2000), Comparison of interglacial stages in the South Atlantic sector of the southern ocean for the past 450 kyr: Implications for marine isotope stage (MIS) 11, *Global Planet. Change*, *24*, 7–26.

Hodell, D. A., C. D. Charles, J. H. Curtis, P. G. Mortyn, U. S. Ninneman, and K. A. Venz (2003), Oxygen isotope stratigraphy of ODP Leg 177 Sites 1088, 1089, 1090, 1093, and 1094, in *Proceedings of the Ocean Drilling Program, Sci. Results*, vol. 177, edited by R. Gersonde, D. A. Hodell, and P. Blum, pp. 1–26, Ocean Drilling Program, College Station, Tex.

Hodell, D. A., J. E. T. Channell, J. H. Curtis, O. E. Romero, and U. Rohl (2008), Onset of "Hudson Strait" Heinrich events in the eastern North Atlantic at the end of the middle Pleistocene transition (~640 ka)?, *Paleoceanography*, *23*, PA4218, doi:10.1029/2008PA001591.

Hodell, D. A., E. K. Minth, J. H. Curtis, I. N. McCave, I. R. Hall, J. E. T. Channell, and C. Xuan (2009), Surface and deep-water hydrography on Gardar Drift (Iceland Basin) during the last interglacial period, *Earth Planet. Sci. Lett.*, *288*, 10–19.

Hodell, D., S. Crowhurst, L. Skinner, P. C. Tzedakis, V. Margari, J. E. T. Channell, G. Kamenov, S. Maclachlan, and G. Rothwell (2013), Response of Iberian Margin sediments to orbital and suborbital forcing over the past 420 ka, *Paleoceanography*, *28*, 185–199, doi:10.1002/palo.20017.

Holbourn, A. E. L., W. Kuhnt, H. Kawamura, Z. Jian, P. M. Grootes, H. Erlenkeuser, and J. Xu (2005), Orbitally-paced paleoproductivity variations in the Timor Sea and Indonesian Throughflow variability during the last 460-ky, *Paleoceanography*, *20*, PA3002, doi:10.1029/2004PA001094.

Hoogakker, B. A. A., I. N. McCave, and M. J. Vautravers (2007), Antarctic link to deep flow speed variation during marine isotope stage 3 in the western North Atlantic, *Earth Planet. Sci. Lett.*, *257*, 463–473.

Hoogakker, B. A. A., M. R. Chapman, I. N. McCave, C. Hillaire-Marcel, C. R. W. Ellison, I. R. Hall, and R. J. Telford (2011), Dynamics of North Atlantic Deep Water masses during the Holocene, *Paleoceanography*, *26*, PA4214, doi:10.1029/2011PA002155.

Hovan, S. A., D. K. Rea, and N. G. Pisias (1991), Late Pleistocene continental climate and oceanic variability recorded in Northwest Pacific sediments, *Paleoceanography*, *6*(3), 349–370, doi:10.1029/91PA00559.

Hüls, M. (2000), Millennial-scale SST variability as inferred from planktonic foraminifera census counts in the western subtropical Atlantic GEOMAR Report 95, GEOMAR Research Center for Marine Geosciences, Christian Albrecht Univ., Kiel.

Hüls, M., and R. Zahn (2000), Millennial-scale sea surface temperature variability in the western tropical North Atlantic from planktonic foraminiferal census counts, *Paleoceanography*, *15*, 659–678, doi:10.1029/1999PA000462.

Imbrie, J. D., A. McIntyre, and A. C. Mix (1989), Oceanic response to orbital forcing in the late Quaternary: Observational and experimental strategies, in *Climate and Geo-Sciences*, edited by A. Berger et al., pp. 121–164, Kluwer Academic, Boston, Mass.

Imbrie, J., and J. Z. Imbrie (1980), Modeling the climatic response to orbital variations, *Science*, *207*, 943–953, doi:10.1126/science.207.4434.943.

Imbrie, J., J. D. Hays, D. G. Martinson, A. McIntyre, A. C. Mix, J. J. Morley, N. G. Pisias, W. L. Prell, and N. J. Shackleton (1984), The orbital theory of Pleistocene climate: Support from a revised chronology, of the marine $\delta^{18}O$ record, in *Milankovitch and Climate, Part 1*, edited by A. Berger, pp. 269–305, Springer, New York.

Imbrie, J., et al. (1992), On the structure and origin of major glaciation cycles: 1. Linear responses to Milankovitch forcing, *Paleoceanography*, *7*, 701–738, doi:10.1029/92PA02253.

Isono, D., M. Yamamoto, T. Irino, T. Oba, M. Murayama, T. Nakamura, and H. Kawahata (2009), The 1500-year climate oscillation in the mid-latitude North Pacific during the Holocene, *Geology*, *37*, 591–594.

Jansen, E., and T. Veum (1990), Evidence for two-step deglaciation and its impact on North Atlantic Deep Water circulation, *Nature*, *343*, 612–616, doi:10.1038/343612a0.

Johnsen, S. J., H. B. Clausen, W. Dansgaard, K. Fuhrer, N. Gundestrup, C. U. Hammer, P. Iverson, J. Jouzel, B. Stauffer, and J. P. Steffenson (1992), Irregular glacial interstadials recorded in a new Greenland ice core, *Nature*, *359*, 311–313, doi:10.1038/359311a0.

Johnsen, S. J., D. Dahl-Jensen, N. Gundestrup, J. P. Steffensen, H. B. Clausen, H. Miller, V. Masson-Delmotte, A. E. Sveinbjörnsdottir, and J. White (2001), Oxygen isotope and palaeotemperature records from six Greenland ice-core stations: Camp Century, Dye-3, GRIP, GISP2, Renland, and NorthGRIP, *J. Quat. Sci.*, *16*, 299–307, doi:10.1002/jqs.622.

Jullien, E., F. E. Grousset, S. R. Hemming, V. L. Peck, I. R. Hall, C. Jeantet, and I. Billy (2006), Contrasting conditions preceding MIS3 and MIS2 Heinrich events, *Global Planet. Change*, *54*(3-4), 225–238, doi:10.1016/j.gloplacha.2006.06.021.

Jung, S. J. A. (1996), Wassermassenaustausch zwischen NE-Atlantik und Nordmeer während der letzten 300,000/80,000 Jahre im Abbild stabiler O- und C- isotope Berichte aus dem Sonderforschungsbereich 313, Christian Albrechts Univ., Kiel.

Kawamura, K., et al. (2007), Northern Hemisphere forcing of climatic cycles in Antarctica over the past 360,000 years, *Nature*, *448*, 912–916, doi:10.1038/nature06015.

Keigwin, L. D. (1995), Stable isotope stratigraphy and chronology of the upper Quaternary section at Site 883, Detroit Seamount, in *Proceedings of the Ocean Drilling Program, Sci. Results*, vol. 145, pp. 257–264, Ocean Drilling Program, College Station, Tex.

Keigwin, L. D., and G. A. Jones (1989), Glacial-Holocene stratigraphy, chronology, and paleoceanographic observations on some North Atlantic sediment drifts, *Deep Sea Res., Part I*, *36*(6), 845–867.

Keigwin, L. D., and G. A. Jones (1994), Western North Atlantic evidence for millennial-scale changes in ocean circulation and climate, *J. Geophys. Res.*, *99*(C6), 12,397–12,410, doi:10.1029/91JC01624.

Keigwin, L. D., G. A. Jones, S. Lehman, and E. Boyle (1991), Deglacial meltwater discharge, North Atlantic deep circulation, and abrupt climate change, *J. Geophys. Res.*, *96*(C9), 16,811–16,826, doi:10.1029/91JC01624.

Keigwin, L. D., W. B. Curry, S. J. Lehman, and S. Johnsen (1994), The role of the deep ocean in North Atlantic climate change between 70 and 130 kyr ago, *Nature*, *371*, 323–325.

Kopp, R. E., F. J. Simons, J. X. Mitrovica, A. C. Maloof, and M. Oppenheimer (2009), Probabilistic assessment of sea level during the last interglacial stage, *Nature*, *462*, 863–867, doi:10.1038/nature08686.

Kopp, R. E., F. J. Simons, J. X. Mitrovica, A. C. Maloof, and M. Oppenheimer (2013), A probabilistic assessment of sea level variations within the last interglacial stage, *Geophys. J. Int.*, *193*, 711–716, doi:10.1093/gji/ggt029.

Labeyrie, L., et al. (1995), Surface and deep hydrology of the Northern Atlantic Ocean during the last 150,000 years, *Philos. Trans. R. Soc. London, Ser. B*, *348*(1324), 255–264.

Labeyrie, L., et al. (1996), Hydrographic changes of the Southern Ocean (southeast Indian sector) over the last 230 kyr, *Paleoceanography*, *11*(1), 57–76, doi:10.1029/95PA02255.

Labeyrie, L., H. Leclaire, C. Waelbroeck, E. Cortijo, J.-C. Duplessy, L. Vidal, M. Elliot, B. Le Coat, and G. Auffret (1999), Temporal variability of the surface and deep waters of the North West Atlantic Ocean at orbital and millennial scales, *Geophys. Monogr. Ser.*, *112*, 77–98, doi:10.1029/GM112p0077.

Labracherie, M., L. D. Labeyrie, J. Duprat, E. Bard, M. Arnold, J. J. Pichon, and J.-C. Duplessy (1989), The last deglaciation in the Southern Ocean, *Paleoceanography*, *4*, 629–638, doi:10.1029/PA004i006p00629.

Lackschewitz, K. S., K.-H. Baumann, B. Gehrke, H.-J. Wallrabe-Adams, J. Thiede, G. Bonani, R. Endler, H. Erlenkeuser, and J. Heinemeier (1998), North Atlantic ice sheet fluctuations 10,000-70,000 yr ago as inferred from deposits on the Reykjanes Ridge, Southeast of Greenland, *Quat. Res.*, *49*, 171–182.

Laj, C., C. Kissel, A. Mazaud, J. E. T. Channell, and J. Beer (2000), North Atlantic palaeointensity stack since 75 ka (NAPIS-75) and the duration of the Laschamp event, *Philos. Trans. R. Soc. London, Ser. A*, *358*, 1009–1025.

Lalicata, J. J., and D. W. Lea (2011), Pleistocene carbonate dissolution fluctuations in the eastern equatorial Pacific on glacial timescales: Evidence from ODP Hole 1241, *Mar. Micropaleontol.*, *79*, 41–51.

Lambeck, K., H. Rouby, A. Purcell, Y. Sun, and M. Sambridge (2014), Sea level and global ice volumes from the Last Glacial Maximum to the Holocene, *Proc. Natl. Acad. Sci. U.S.A.*, *111*, 15,296–15,303.

Landais, A., et al. (2013), Two-phase change in CO_2, Antarctic temperature and global climate during Termination II, *Nat. Geosci.*, *6*, 1062–1065, doi:10.1038/NGEO1985.

Larsen, N. K., K. L. Knudsen, C. F. O. G. Krohn, C. Kronborg, A. S. Murray, and O. B. Nielsen (2009), Late Quaternary ice sheet, lake and sea history of southwest Scandanavia—A synthesis, *Boreas*, *38*, 732–761, doi:10.1111/j.1502-3885.2009.00101.x.

Laskar, J., P. Robutel, F. Joutel, M. Gastineau, A. C. M. Correia, and B. Levrard (2004), A long-term numerical solution for the insolation quantities of the Earth, *Astron. Astrophys.*, *428*, 261–285, doi:10.1051/0004-6361:20041335.

Lea, D. W., P. A. Martin, D. K. Pak, and H. J. Spero (2002), Reconstructing a 350 ky history of sea level using planktonic Mg/Ca and oxygen isotope records from a Cocos Ridge core, *Quat. Sci. Rev.*, *21*, 283–293.

Lea, D. W., D. K. Pak, C. L. Belanger, H. J. Spero, M. A. Hall, and N. J. Shackleton (2006), Paleoclimate history of Galápagos surface waters over the last 135,000 yr, *Quat. Sci. Rev.*, *25*, 1152–1167, doi:10.1016/j.quascirev.2005.11.010.

Lebreiro, S. M., A. H. L. Voelker, A. Vizcaino, F. G. Abrantes, U. Alt-Epping, S. Jung, N. Thouvenye, and E. Gràcia (2009), Sediment instability on the Portuguese continental margin under abrupt glacial climate changes (last 60 kyr), *Quat. Sci. Rev.*, *28*(27-28), 3211–3223, doi:10.1016/j.quascirev.2009.08.007.

Lee, M. Y., K. Y. Wei, and Y. G. Chen (1999), High resolution oxygen isotope stratigraphy for the last 150,000 years in the southern South China Sea: Core MD972151, *Terr. Atmos. Oceanic Sci.*, *10*, 239–254.

Lisiecki, L. E., and M. E. Raymo (2005), A Pliocene-Pleistocene stack of 57 globally distributed benthic $\delta^{18}O$ records, *Paleoceanography*, *20*, PA1003, doi:10.1029/2004PA001071.

Lisiecki, L. E., and M. E. Raymo (2009), Diachronous benthic $\delta^{18}O$ responses during late Pleistocene terminations, *Paleoceanography*, *24*, PA3210, doi:10.1029/2009PA001732.

Lisiecki, L. E., and P. A. Lisiecki (2002), Application of dynamic programming to the correlation of paleoclimate records, *Paleoceanography*, *17*(D4), 1049, doi:10.1029/2001PA000733.

Lisiecki, L. E., M. E. Raymo, and W. B. Curry (2008), Atlantic overturning responses to late Pleistocene climate forcings, *Nature*, *456*, 85–88, doi:10.1038/nature07425.

Little, M. G., R. R. Schneider, D. Kroon, B. Price, T. Bickert, and G. Wefer (1997), Rapid paleoceanographic changes in the Benguela upwelling system for the last 160,000 years as indicated by abundances of planktonic foraminifera, *Palaeogeogr. Palaeoclim. Palaeoecol.*, *130*, 135–161.

Loubere, P., M. Richaud, Z. Liu, and F. Mekik (2003), Oceanic conditions in the eastern equatorial Pacific during the onset of ENSO in the Holocene, *Quat. Res.*, *60*, 142–148.

Lourantou, A., J. Chappellaz, J.-M. Barnola, V. Masson-Delmotte, and D. Raynaud (2010), Changes in atmospheric CO_2 and its carbon isotopic ratio during the penultimate deglaciation, *Quat. Sci. Rev.*, *29*, 1983–1992.

Lyle, M., R. Zahn, F. Prahl, J. Dymond, R. Collier, N. Pisias, and E. Suess (1992), Paleoproductivity and carbon burial across the California Current: The multitracers transect, 42°N, *Paleoceanography*, *7*, 251–272, doi:10.1029/92PA00696.

Lyle, M., A. Mix, A. C. Ravelo, D. Andreasen, L. Heusser, and A. Olivarez (2000), Millennial scale $CaCO_3$ and Corg events along the northern and central California margin: Stratigraphy and origins, in *Proceedings of the Ocean Drilling Program, Sci. Results*, vol. 167, edited by M. Lyle et al., pp. 163–182, Ocean Drilling Program, College Station, Tex., doi:10.2973/odp.proc.sr.167.214.2000.

Lyle, M., A. Mix, and N. Pisias (2002), Patterns of $CaCO_3$ deposition in the eastern tropical Pacific Ocean for the last 150 kyr: Evidence for a southeast Pacific depositional spike during marine isotope stage (MIS) 2, *Paleoceanography*, *17*(2), 1013, doi:10.1029/2000PA000538.

Mackensen, A., and T. Bickert (1999), Stable carbon isotopes in benthic foraminifera: Proxies for deep and bottom water circulation and new production, in *Use of Proxies in Paleoceanography—Examples from the South Atlantic*, edited by G. Fischer and G. Wefer, pp. 229–254, Springer, Berlin, Heidelberg.

Mackensen, A., H. Grobe, H. W. Hubberten, and G. Kuhn (1994), Benthic foraminiferal assemblages and the $\delta^{13}C$-signal in the Atlantic sector of the Southern Ocean: Glacial-interglacial contrasts, in *Carbon Cycling in the Glacial Ocean: Constraints on the Ocean's Role in Global Change*, edited by R. Zahn et al., pp. 105–114, Springer, Berlin.

Mackensen, A., M. Rudolph, and G. Kuhn (2001), Late Pleistocene deep-water circulation in the subantarctic eastern Atlantic, *Global Planet. Change*, *30*, 197–229, doi:10.1016/S0921-8181(01)00102-3.

Marchitto, T. M., J. Lynch-Stieglitz, and S. R. Hemming (2005), Deep Pacific $CaCO_3$ compensation and glacial–interglacial atmospheric CO_2, *Earth Planet. Sci. Lett.*, *231*, 317–336.

Marcott, S. A., et al. (2011), Ice-shelf collapse from subsurface warming as a trigger for Heinrich events, *Proc. Natl. Acad. Sci. U.S.A.*, *108*(33), 13,415–13,419, doi:10.1073/pnas.1104772108.

Marcott, S. A., et al. (2014), Centennial-scale changes in the global carbon cycle during the last deglaciation, *Nature*, *515*, 616–619, doi:10.1038/nature13799.

Marino, G., E. J. Rohling, L. Rodríguez-Sanz, K. M. Grant, D. Heslop, A. P. Roberts, J. D. Stanford, and J. Yu (2015), Bipolar seesaw control on last interglacial sea level, *Nature*, *522*, 197–201.

Martin, P. A., D. W. Lea, Y. Rosenthal, N. J. Shackleton, M. Sarnthein, and T. Papenfuss (2002), Quaternary deep sea temperature histories derived from benthic foraminiferal Mg/Ca, *Earth Planet. Sci. Lett.*, *198*, 193–209.

Martinson, D. G., N. G. Pisias, J. D. Hays, J. Imbrie, T. C. Moore, and N. J. Shackleton (1987), Age dating and the orbital theory of the ice ages: Development of a high-resolution 0 to 300,000-year chronostratigraphy, *Quat. Res.*, *27*(1), 1–29.

Masson-Delmotte, V., et al. (2010), EPICA Dome C record of glacial and interglacial intensities, *Quat. Sci. Rev.*, *29*, 113–128.

McIntyre, A., W. F. Ruddiman, K. Karlin, and A. C. Mix (1989), Surface water response of the equatorial Atlantic Ocean to orbital forcing, *Paleoceanography*, *4*, 19–55, doi:10.1029/PA004i001p00019.

McManus, J. F., D. W. Oppo, and J. L. Cullen (1999), A 0.5-million-year record of millennial-scale climate variability in the North Atlantic, *Science*, *283*(5404), 971–975, doi:10.1126/science.283.5404.971.

McManus, J. F., R. Francois, J. Gherardi, L. Keigwin, and S. Brown-Leger (2004), Collapse and rapid resumption of Atlantic meridional circulation linked to deglacial climate changes, *Nature*, *428*(6985), 834–837, doi:10.1038/nature02494.

Medina-Elizalde, M. (2013), A global compilation of coral sea-level benchmarks: Implications and new challenges, *Earth Planet. Sci. Lett.*, *362*, 310–318, doi:10.1016/j.epsl.2012.12.001.

Millo, C., M. Sarnthein, A. Voelker, and H. Erlenkeuser (2006), Variability of the Denmark Strait Overflow during the Last Glacial Maximum, *Boreas*, *35*, 50–60.
Mix, A. C. (1986), Late Quaternary paleoceanography of the Atlantic Ocean: Foraminiferal faunal and stable-isotopic evidence, PhD thesis, 321 pp., Columbia Univ.
Mix, A. C., and R. G. Fairbanks (1985), North Atlantic surface-ocean control of Pleistocene deep-ocean circulation, *Earth Planet. Sci. Lett.*, *73*, 231–243.
Mix, A. C., N. G. Pisias, R. Zahn, W. Rugh, C. Lopez, and K. Nelson (1991), Carbon 13 in Pacific deep and intermediate waters, 0-370 ka: Implications for ocean circulation and Pleistocene CO_2, *Paleoceanography*, *6*, 205–226, doi:10.1029/90PA02303.
Mix, A. C., J. Le, and N. J. Shackleton (1995a), Benthic foraminiferal stable isotope stratigraphy of Site 846: 0-1.8 Ma, in *Proceedings of the Ocean Drilling Program*, *Sci. Results*, vol. 138, edited by N. G. Pisias et al., pp. 839–854, Ocean Drilling Program, College Station, Tex.
Mix, A. C., N. G. Pisias, W. Rugh, J. Wilson, A. E. Morey, and T. Hagelberg (1995b), Benthic foraminifer stable isotope record from Site 849 (0-5 Ma): Local and global climate changes, in *Proceedings of the Ocean Drilling Program*, *Sci. Results*, vol. 138, pp. 371–412, Ocean Drilling Program, College Station, Tex., doi:10.2973/odp.proc.sr.138.120.1995.
Mix, A., and W. Ruddiman (1984), Oxygen-isotope analyses and Pleistocene ice volumes, *Quat. Res.*, *21*(1), 1–20, doi:10.1016/0033-5894(84)90085-1.
Mohtadi, M., D. Hebbeln, S. N. Ricardo, and C. B. Lange (2006), El Niño-like pattern in the Pacific during marine isotope stages (MIS) 13 and 11?, *Paleoceanography*, *21*, PA1015, doi:10.1029/2005PA001190.
Mojtahid, M., F. Eynaud, S. Zaragosi, J. Scourse, J.-F. Bourillet, and T. Garlan (2005), Palaeoclimatology and palaeohydrography of the glacial stages on Celtic and Armorican margins over the last 360,000 yrs, *Mar. Geol.*, *224*(1-4), 57–82, doi:10.1016/j.margeo.2005.07.007.
Molyneux, E. G., I. R. Hall, R. Zahn, and P. Diz (2007), Deep water variability on the southern Agulhas Plateau: Interhemispheric links over the past 170 ka, *Paleoceanography*, *22*, PA4209, doi:10.1029/2006PA001407.
Mortyn, P. G., R. C. Thunell, D. M. Anderson, L. D. Stott, and J. Le (1996), Sea surface temperature changes in the Southern California Borderlands during the last glacial-interglacial cycle, *Paleoceanography*, *11*(4), 415–430, doi:10.1029/96PA01236.
Mulitza, S., M. Prange, J.-B. Stuut, M. Zabel, T. von Dobeneck, A. C. Itambi, J. Nizou, M. Schulz, and G. Wefer (2008), Sahel megadroughts triggered by glacial slowdown of Atlantic meridional overturning, *Paleoceanography*, *23*, PA4206, doi:10.1029/2008PA001637.
Murray, R. W., C. Knowlton, M. Leinen, A. C. Mix, and C. H. Polsky (2000), Export production and carbonate dissolution in the central equatorial Pacific Ocean over the past 1 Ma, *Paleoceanography*, *15*, 570–592, doi:10.1029/1999PA000457.
NEEM community members (2013), Eemian interglacial reconstructed from a Greenland folded ice core, *Nature*, *493*, 489–494, doi:10.1038/nature11789.
Nelson, C. S., C. H. Hendy, A. M. Cuthbertson, and G. R. Jarrett (1986), Late Quaternary carbonate and isotope stratigraphy, subantarctic Site 594, Southwest Pacific, *Initial Rep. Ocean Drill. Proj.*, *90*, 1425–1436, doi:10.2973/dsdp.proc.90.144.1986.
Nelson, C. S., P. J. Cooke, C. H. Hendy, and A. M. Cuthbertson (1993), Oceanographic and climatic changes over the past 160,000 years at Deep Sea Drilling Project Site 594 off southeastern New Zealand, southwest Pacific Ocean, *Paleoceanography*, *8*, 435–458, doi:10.1029/93PA01162.
Ninkovitch, D., and N. J. Shackleton (1975), Distribution, stratigraphic position and age of ash layer "L," in the Panama Basin region, *Earth Planet. Sci. Lett.*, *27*, 20–34.
North Greenland Ice Core Project Members (2004), High-resolution record of Northern Hemisphere climate extending into the last interglacial period, *Nature*, *431*(7005), 147–151, doi:10.1038/nature02805.
Nürnberg, D., N. Brughmans, J. Schönfeld, U. Ninnemann, and C. Dullo (2004), Paleo-export productivity, terrigenous flux, and sea surface temperature around Tasmania—Implications for glacial/interglacial changes in the Subtropical Convergence Zone, *Geophys. Monogr. Ser.*, *151*, 291–318.
Oba, T., and M. Murayama (2004), Sea-surface temperature and salinity changes in the northwest Pacific since the Last Glacial Maximum, *J. Quat. Sci.*, *19*(4), 335–346.
Oba, T., T. Irino, M. Yamamoto, M. Murayama, A. Takamura, and K. Aoki (2006), Paleoceanographic change off central Japan since the last 144,000 years based on high-resolution oxygen and carbon isotope records, *Global Planet. Change*, *53*, 5–20.
Ohkushi, K., A. Suzuki, H. Kawahata, and L. P. Gupta (2003), Glacial-interglacial deep-water changes in the NW Pacific inferred from single foraminiferal $\delta^{18}O$ and $\delta^{13}C$, *Mar. Micropaleontol.*, *48*, 281–290.
Oppo, D. W., and M. Horowitz (2000), Glacial deep water geometry: South Atlantic benthic foraminiferal Cd/Ca and $\delta^{13}C$ evidence, *Paleoceanography*, *15*(2), 147–160, doi:10.1029/1999PA000436.
Oppo, D. W., and R. G. Fairbanks (1987), Variability in the deep and intermediate water circulation of the Atlantic Ocean during the past 25,000 years: Northern Hemisphere modulation of the Southern Ocean, *Earth Planet. Sci. Lett.*, *86*, 1–15, doi:10.1016/0012-821X(87)90183-X.
Oppo, D. W., and R. G. Fairbanks (1990), Atlantic Ocean thermohaline circulation of the last 150,000 years: Relationship to climate and atmospheric CO_2, *Paleoceanography*, *5*, 277–288, doi:10.1029/PA005i003p00277.
Oppo, D. W., and S. J. Lehman (1995), Suborbital timescale variability of North Atlantic Deep Water during the past 200,000 years, *Paleoceanography*, *10*(5), 901–910, doi:10.1029/95PA02089.
Oppo, D. W., and Y. Sun (2005), Amplitude and timing of sea-surface temperature change in the northern South China Sea: Dynamic link to the East Asian monsoon, *Geology*, *33*, 785–788.
Oppo, D. W., R. G. Fairbanks, A. L. Gordon, and N. J. Shackleton (1990), Late Pleistocene Southern Ocean $\delta^{13}C$ variability, *Paleoceanography*, *5*, 43–54, doi:10.1029/PA005i001p00043.
Oppo, D. W., M. Horowitz, and S. J. Lehman (1997), Marine core evidence for reduced deep water production during Termination II followed by a relatively stable substage 5e (Eemian), *Paleoceanography*, *12*, 51–63, doi:10.1029/96PA03133.
Oppo, D. W., L. D. Keigwin, J. F. McManus, and J. L. Cullen (2001), Persistent suborbital climate variability in marine isotope stage 5 and Termination II, *Paleoceanography*, *16*(3), 280–292, doi:10.1029/2000PA000527.
Ostermann, D. R., and W. B. Curry (2000), Calibration of stable isotopic data: An enriched $\delta^{18}O$ standard used for source gas mixing detection and correction, *Paleoceanography*, *15*(3), 353–360, doi:10.1029/1999PA000411.
Pahnke, K., and R. Zahn (2005), Southern Hemisphere water mass conversion linked with North Atlantic climate variability, *Science*, *307*, 1741–1746, doi:10.1126/science.1102163.
Pahnke, K., R. Zahn, H. Elderfield, and M. Schulz (2003), 340,000-year centennial-scale marine record of Southern Hemisphere climatic oscillation, *Science*, *301*, 948–952, doi:10.1126/science.1084451.
Pailler, D., and E. Bard (2002), High frequency palaeoceanographic changes during the past 140,000 yr recorded by the organic matter in sediments of the Iberian Margin, *Palaeogeogr. Palaeoclimatol. Palaeoecol.*, *181*, 431–452, doi:10.1016/S0031-0182(01)00444-8.

Parrenin, F., and D. Paillard (2012), Terminations VI and VIII (~530 and ~720 kyr BP) tell us the importance of obliquity and precession in the triggering of deglaciations, *Clim. Past*, *8*, 2031–2037, doi:10.5194/cp-8-2031-2012.
Parrenin, F., et al. (2007), The EDC3 chronology for the EPICA Dome C ice core, *Clim. Past*, *3*, 485–497, doi:10.5194/cp-3-485-2007.
Petit, J. R., et al. (1999), Climate and atmospheric history of the past 420,000 years from the Vostok ice core, Antarctica, *Nature*, *399*, 429–436, doi:10.1038/20859.
Pichevin, L., P. Martinez, P. Bertrand, R. Schneider, and J. Giraudeau (2005), Nitrogen cycling on the Namibian shelf and slope over the last two climatic cycles: Local and global forcings, *Paleoceanography*, *20*, PA2006, doi:10.1029/2004PA001001.
Pichon, J. L., L. Labeyrie, G. F. Bareille, M. Labracherie, J. Duprat, and J. Jouzel (1992), Surface water temperature changes in the high latitudes of the southern hemisphere over the last glacialinterglacial cycle, *Paleoceanography*, *7*, 289–318, doi:10.1029/92PA00709.
Pierre, C., J. F. Saliege, M. J. Urrutiaguer, and J. Giraudeau (2001), Stable isotope record of the last 500 k.y. at Site 1087 (Southern Cape Basin), in *Proceedings of the Ocean Drilling Program*, *Sci. Results*, vol. 175, pp. 1–22, Ocean Drilling Program, College Station, Tex., doi:10.2973/odp.proc.sr.175.230.2001.
Piotrowski, A. M., S. L. Goldstein, S. R. Hemming, and R. G. Fairbanks (2004), Intensification and variability of ocean thermohaline circulation through the last deglaciation, *Earth Planet. Sci. Lett.*, *225*, 205–220.
Pisias, N., and A. Mix (1997), Spatial and temporal oceanographic variability of the eastern equatorial Pacific during the late Pleistocene: Evidence from radiolaria microfossils, *Paleoceanography*, *12*, 381–393, doi:10.1029/97PA00583.
Pisias, N. G., D. G. Martinson, T. C. Moore Jr., N. J. Shackleton, W. Prell, J. Hays, and G. Boden (1984), High resolution stratigraphic correlation of benthic oxygen isotope records spanning the last 300,000 years, *Mar. Geol.*, *56*, 119–136.
Praetorius, S. K., J. F. McManus, D. W. Oppo, and W. B. Curry (2008), Episodic reductions in bottom-water currents since the last ice age, *Nat. Geosci.*, *1*, 449–452.
Rashid, H., R. Hesse, and D. J. W. Piper (2003), Evidence for an additional Heinrich event between H5 and H6 in the Labrador Sea, *Paleoceanography*, *18*(4), 1077, doi:10.1029/2003PA000913.
Raymo, M. E., D. W. Oppo, and W. Curry (1997), The mid-Pleistocene climate transition: A deep sea carbon isotopic perspective, *Paleoceanography*, *12*(4), 546–559, doi:10.1029/97PA01019.
Raymo, M. E., D. W. Oppo, B. P. Flower, D. A. Hodell, J. F. McManus, K. A. Venz, K. F. Kleiven, and K. McIntyre (2004), Stability of North Atlantic water masses in face of pronounced climate variability during the Pleistocene, *Paleoceanography*, *19*, PA2008, doi:10.1029/2003PA000921.
Raymo, M. E., L. E. Lisiecki, and K. H. Nisancioglu (2006), Plio-Pleistocene ice volume, Antarctic climate, and the global $\delta^{18}O$ record, *Science*, *313*, doi:10.1126/science.1123296.
Reimer, P. J., et al. (2013), Intcal13 and Marine13 radiocarbon age calibration curves 0-50,000 years cal BP, *Radiocarbon*, *55*, 1869–1887.
Richter, T. (1998), Sedimentary fluxes at the Mid-Atlantic Ridge—Sediment sources, accumulation rates, and geochemical characterisation GEOMAR Report 73, GEOMAR Research Center for Marine Geosciences, Christian Albrechts University, Kiel.
Rohling, E. J., K. Grant, M. Bolshaw, A. P. Roberts, M. Siddall, C. Hemleben, and M. Kucera (2009), Antarctic temperature and global sea level closely coupled over the past five glacial cycles, *Nat. Geosci.*, *2*, 500–504, doi:10.1038/ngeo557.
Rohling, E. J., et al. (2014), Sea-level and deep-sea-temperature variability over the past 5.3 million years, *Nature*, *508*, 477–482.
Röthlisberger, R., et al. (2008), The Southern Hemisphere at glacial terminations: Insights from the Dome C ice core, *Clim. Past*, *4*, 345–356.
Ruddiman, W. F., and A. McIntyre (1981), Oceanic mechanism for amplification of the 23,000 year ice-volume cycle, *Science*, *212*, 617–627.
Ruddiman, W. F., B. Molfino, A. Esmay, and E. Pokras (1980), Evidence bearing on the mechanism of rapid deglaciation, *Clim. Change*, *3*, 65–87, doi:10.1007/BF02423169.
Rühlemann, C., S. Mulitza, P. M. Muller, G. Wefer, and R. Zahn (1999), Warming of the tropical Atlantic Ocean and slowdown of thermohaline circulation during the last deglaciation, *Nature*, *402*, 511–514.
Rühlemann, C., S. Mulitza, G. Lohmann, A. Paul, M. Prange, and G. Wefer (2004), Intermediate depth warming in the tropical Atlantic related to weakened thermohaline circulation: Combining paleoclimate data and modeling results for the last deglaciation, *Paleoceanography*, *19*, PA1025, doi:10.1029/2003PA000948.
Russon, T., M. Elliot, C. Kissel, G. Cabioch, P. De Deckker, and T. Corrège (2009), Middle-late Pleistocene deep water circulation in the southwest subtropical Pacific, *Paleoceanography*, *24*, PA4205, doi:10.1029/2009PA001755.
Ruth, U., et al. (2007), "EDML1": A chronology for the EPICA deep ice core from Dronning Maud Land, Antarctica, over the last 150,000 years, *Clim. Past*, *3*, 475–484, doi:10.5194/cp-3-475-2007.
Saikku, R., L. Stott, and R. Thunell (2009), A bi-polar signal recorded in the western tropical Pacific: Northern and Southern Hemisphere climate records from the Pacific warm pool during the Last Ice Age, *Quat. Sci. Rev.*, *28*, 2374–2385, doi:10.1016/j.quascirev.2009.05.007.
Salgueiro, E., A. H. L. Voelker, L. de Abreu, F. Abrantes, H. Meggers, and G. Wefer (2010), Temperature and productivity changes off the western Iberian margin during the last 150 kyr, *Quat. Sci. Rev.*, *29*(5-6), 680–695, doi:10.1016/j.quascirev.2009.11.013.
Samson, C. R., E. L. Sikes, and W. R. Howard (2005), Deglacial paleoceanographic history of the Bay of Plenty, New Zealand, *Paleoceanography*, *20*, PA4017, doi:10.1029/2004PA001088.
Sanchez-Goni, M. F., M. F. Loutre, M. Crucifix, O. Peyron, L. Santos, J. Duprat, B. Malaizé, J.-L. Turon, and J.-P. Peypouquet (2005), Increasing vegetation and climate gradient in western Europe over the Last Glacial Inception (122–110 ka): Data-model comparison, *Earth Planet. Sci. Lett.*, *231*(1-2), 111–130.
Sanchez-Goni, M. F., et al. (2012), European climate optimum and enhanced Greenland melt during the Last Interglacial, *Geology*, *40*, 627–630.
Sarnthein, M., K. Winn, S. J. A. Jung, J.-C. Duplessy, L. Labeyrie, H. Erlenkeuser, and G. Ganssen (1994), Changes in east Atlantic deepwater circulation over the last 30,000 years: Eight time slice reconstructions, *Paleoceanography*, *9*(2), 209–267, doi:10.1029/93PA03301.
Sarnthein, M., H. Gebhardt, T. Kiefer, M. Kucera, M. Cook, and H. Erlenkeuser (2004), Mid-Holocene origin of the sea surface salinity low in the subarctic North Pacific, *Quat. Sci. Rev.*, *23*, 2089–2099.
Sarnthein, M., H. Gebhardt, T. Kiefer, H. Erlenkeuser, C. Kissel, and F. Schmieder (2005), 95-Ky cycles of ocean circulation in the far northwestern Pacific and South China Sea during the Brunhes Chron, in *Milutin Milankovitch Anniversary Symposium: Paleoclimate and the Earth Climate System, Serbian Academy of Sciences and Arts, 110*, edited by A. Berger et al., pp. 135–140, Serbian Acad. of Sci. and Arts, Belgrade.
Sarnthein, M., P. Grootes, J. Kennett, and M.-J. Nadeau (2007), ^{14}C reservoir ages show deglacial changes in ocean currents and carbon cycle, *Geophys. Monogr. Ser.*, *173*, 175–196, doi:10.1029/173GM13.
Sarnthein, M., P. M. Grootes, A. Holbourn, W. Kuhnt, and H. Kuhn (2011), Tropical warming in the Timor Sea led deglacial Antarctic warming and atmospheric CO_2 rise by more than 500 yr, *Earth Planet. Sci. Lett.*, *302*, 337–348, doi:10.1016/j.epsl.2010.12.021.
Sarnthein, M., H. Sadatzki, and Z. M. Jian (2013), Stratigraphic gaps at northern South China Sea margin reflect changes in Pacific deepwater inflow at glacial Termination II, *Sci. China Earth Sci.*, *56*(10), 1748–1758, doi:10.1007/s11430-013-4678-2.

Schlünz, B., R. Schneider, P. J. Müller, and G. Wefer (2000), Late Quaternary organic carbon accumulation south of Barbados: Influence of the Orinoco and Amazon rivers?, *Deep Sea Res., Part I*, *47*, 1101–1124.
Schmiedl, G., and A. Mackensen (1997), Late Quaternary paleoproductivity and deep water circulation in the eastern South Altantic Ocean: Evidence from benthic foraminifera, *Palaeogeogr. Palaeoclimatol. Palaeoecol.*, *130*, 43–80.
Schmiedl, G., and A. Mackensen (2006), Multispecies stable isotopes of benthic foraminifers reveal past changes of organic matter decomposition and deepwater oxygenation in the Arabian Sea, *Paleoceanography*, *21*, PA4213, doi:10.1029/2006PA001284.
Schönfeld, J., R. Zahn, and L. de Abreu (2003), Surface and deep water response to rapid climate changes at the Western Iberian Margin, *Global Planet. Change*, *36*(4), 237–264, doi:10.1016/S0921-8181(02)00197-2.
Shackleton, N. J. (1977), Carbon-13 in Uvigerina: Tropical rain forest history and the equatorial Pacific carbonate dissolution cycle, in *The Fate of Fossil Fuel in the Oceans*, edited by N. R. Andersen and A. Malahoff, pp. 401–427, Plenum Press, New York.
Shackleton, N. J., and M. A. Hall (1989), Stable isotope history of the Pleistocene at ODP Site 677, in *Proceedings of the Ocean Drilling Program, Sci. Results*, vol. 111, edited by K. Becker and H. Sakai, pp. 295–316, Ocean Drilling Program, College Station, Tex.
Shackleton, N. J., J. Imbrie, and M. A. Hall (1983), Oxygen and carbon isotope record of East Pacific core V19-30: Implications for the formation of deep water in the late Pleistocene North Atlantic, *Earth Planet. Sci. Lett.*, *65*, 233–244.
Shackleton, N. J., A. Berger, and W. R. Peltier (1990), An alternative astronomical calibration of the lower Pleistocene timescale based on ODP Site 677, *Trans. R. Soc. Edinburgh: Earth Sci.*, *81*, 251–261.
Shackleton, N. J., M. A. Hall, and E. Vincent (2000), Phase relationships between millennial-scale events 64,000-24,000 years ago, *Paleoceanography*, *115*(6), 565–569, doi:10.1029/2000PA000513.
Shackleton, N. J., R. G. Fairbanks, T. Chiu, and F. Parrenin (2004), Absolute calibration of the Greenland time scale: Implications for Antarctic time scales and for $\Delta^{14}C$, *Quat. Sci. Rev.*, *23*(14-15), 1513–1522, doi:10.1016/j.quascirev.2004.03.006.
Shakun, J. D., P. U. Clark, F. He, S. A. Marcott, A. C. Mix, Z. Liu, B. Otto-Bliesner, A. Schmittner, and E. Bard (2012), Global warming preceded by increasing carbon dioxide concentrations during the last deglaciation, *Nature*, *484*(7392), 49–54, doi:10.1038/nature10915.
Shakun, J. D., D. W. Lea, L. E. Lisiecki, and M. E. Raymo (2015), An 800-kyr record of global surface ocean $\delta^{18}O$ and implications for ice volume-temperature coupling, *Earth Planet. Sci. Lett.*, *426*, 58–68.
Siberlin, C., and C. Wunsch (2011), Oceanic tracer and proxy time scales revisited, *Clim. Past*, *7*, 27–39, doi:10.5194/cp-7-27-2011.
Siddall, M., E. Bard, E. J. Rohling, and C. Hemleben (2006), Sea-level reversal during Termination II, *Geology*, *34*, 17–820, doi:10.1130/G22705.1.
Siddall, M., E. J. Rohling, W. G. Thompson, and C. Waelbroeck (2008), Marine isotope stage 3 sea level fluctuations: Data synthesis and new outlook, *Rev. Geophys.*, *46*, RG4003, doi:10.1029/2007RG000226.
Sierro, F. J., et al. (2009), Phase relationship between sea level and abrupt climate change, *Quat. Sci. Rev.*, *28*, 2867–2881.
Sikes, E. L., W. R. Howard, C. R. Samson, T. S. Mahan, L. G. Robertson, and J. K. Volkman (2009), Southern Ocean seasonal temperature and Subtropical Front movement on the South Tasman Rise in the late Quaternary, *Paleoceanography*, *24*, PA2201, doi:10.1029/2008PA001659.
Sirocko, F., M. Sarnthein, H. Erlenkeuser, H. Lange, M. Arnold, and J.-C. Duplessy (1993), Century-scale events in monsoonal climate over the past 24,000 years, *Nature*, *364*, 322–324.
Sirocko, F., D. Garbe-Schonberg, and C. Devey (2000), Processes controlling trace element geochemistry of Arabian Sea sediments during the last 25,000 years, *Global Planet. Change*, *26*, 217–303.
Skinner, L. C., and H. Elderfield (2007), Rapid fluctuations in the deep North Atlantic heat budget during the last glacial period, *Paleoceanography*, *22*, PA1205, doi:10.1029/2006PA001338.
Skinner, L. C., and N. J. Shackleton (2004), Rapid transient changes in northeast Atlantic deep water ventilation age across Termination I, *Paleoceanography*, *19*, PA2005, doi:10.1029/2003PA000983.
Skinner, L. C., and N. J. Shackleton (2005), An Atlantic lead over Pacific deep-water change across Termination I: Implications for the application of the marine isotope stage stratigraphy, *Quat. Sci. Rev.*, *24*(5-6), 571–580, doi:10.1016/j.quascirev.2004.11.008.
Skinner, L. C., and N. J. Shackleton (2006), Deconstructing Terminations I and II: Revisiting the glacioeustatic paradigm based on deep-water temperature estimates, *Quat. Sci. Rev.*, *25*, 3312–3321, doi:10.1016/j.quascirev.2006.07.005.
Skinner, L. C., N. J. Shackleton, and H. Elderfield (2003), Millennial-scale variability of deep-water temperature and $\delta^{18}O_{dw}$ indicating deep-water source variations in the Northeast Atlantic, 0-34 cal. ka BP, *Geochem. Geophys. Geosyst.*, *4*(12), 1098, doi:10.1029/2003GC000585.
Skinner, L. C., S. Fallon, C. Waelbroeck, E. Michel, and S. Barker (2010), Ventilation of the deep Southern Ocean and deglacial CO_2 rise, *Science*, *328*, 1147–1151, doi:10.1126/science.1183627.
Slowey, N. C., and W. B. Curry (1995), Glacial-interglacial differences in circulation and carbon cycling within the upper western North Atlantic, *Paleoceanography*, *10*, 715–732, doi:10.1029/95PA01166.
Smart, C. W., C. Waelbroeck, E. Michel, and A. Mazaud (2010), Benthic foraminiferal abundance and stable isotopic changes in the Indian Ocean sector of the Southern Ocean during the last 20 kyr: Paleoceanographic implications, *Palaeogeogr. Palaeoclimatol. Palaeoecol.*, *297*, 537–548.
Smith, D. E., S. Harrison, C. R. Firth, and J. T. Jordan (2011), The early Holocene sea level rise, *Quat. Sci. Rev.*, *30*, 1846–1860, doi:10.1016/j.quascirev.2011.04.019.
Sosdian, S., and Y. Rosenthal (2009), Dee-sea temperature and ice volume changes across the Pliocene-Pleistocene climate transitions, *Science*, *325*, 306–310, doi:10.1126/science.1169938.
Southon, J., A. L. Noronha, H. Cheng, R. L. Edwards, and Y. Wang (2012), A high-resolution record of atmospheric ^{14}C based on Hulu Cave speleothem H82, *Quat. Sci. Rev.*, *33*, 32–41, doi:10.1026/j.quascirev.2011.11.022.
Sowers, T., M. L. Bender, L. Labeyrie, D. G. Martinson, J. Jouzel, D. Raynaud, J. J. Pichon, and Y. S. Korotkevich (1993), A 135,000-year Vostok-SPECMAP common temporal framework, *Paleoceanography*, *8*, 737–766, doi:10.1029/93PA02328.
Speed, R. C., and H. Cheng (2004), Evolution of marine terraces and sea level in the last interglacial, Cave Hill, Barbados, *GSA Bull.*, *116*(1-2), 219–232, doi:10.1130/B25167.1.
Spratt, R. M., and L. E. Lisiecki (2016), A late Pleistocene sea level stack, *Clim. Past*, *12*, 1079–1092, doi:10.5194/cp-12-1079-2016.
Stein, M., G. J. Wasserburg, P. Aharon, J. H. Chen, Z. R. Zhu, A. Bloom, and J. Chappell (1993), TIMS U-series dating and stable isotopes of the last interglacial event in Papua New Guinea, *Geochim. Cosmochim. Acta*, *57*, 2541–2554, doi:10.1016/0016-7037(93)90416-T.
Stern, J. V., and L. E. Lisiecki (2013), North Atlantic circulation and reservoir age changes over the past 41,000 years, *Geophys. Res. Lett.*, *40*, 3693–3697, doi:10.1002/grl.50679.
Stern, J. V., and L. E. Lisiecki (2014), Termination 1 timing in radiocarbon-dated regional benthic $\delta^{18}O$ stacks, *Paleoceanography*, *29*, 1127–1142, doi:10.1002/2014PA002700.
Stirling, C. H., T. M. Esat, K. Lambeck, and M. T. McCulloch (1998), Timing and duration of the last interglacial: Evidence for a restricted interval of widespread coral reef growth, *Earth Planet. Sci. Lett.*, *160*, 745–762, doi:10.1016/S0012-821X(98)00125-3.

Stocker, T. F., and S. J. Johnsen (2003), A minimum thermodynamic model for the bipolar seesaw, *Paleoceanography*, *18*(4), 1087, doi:10.1029/2003PA000920.
Storey, M., R. G. Roberts, and M. Saidin (2012), Astronomically calibrated Ar-40/Ar-39 age for the Toba supereruption and global synchronization of late Quaternary records, *Proc. Natl. Acad. Sci. U.S.A.*, *109*, 18,684–18,688, doi:10.1073/pnas.1208178109.
Stott, L. D. (2007), Comment on "Anomalous radiocarbon ages for foraminifera shells" by W. Broecker et al.: A correction to the western tropical Pacific MD9821-81 record, *Paleoceanography*, *22*, PA1211, doi:10.1029/2006PA001379.
Stott, L. D., M. Nuemann, and D. Hammond (2000), Intermediate water ventilation on the northeastern Pacific margin during the late Pleistocene inferred from benthic foraminiferal $\delta^{13}C$, *Paleoceanography*, *15*, 161–169, doi:10.1029/1999PA000375.
Stott, L. D., A. Timmermann, and R. Thunell (2007), Southern Hemisphere and deep-sea warming led deglacial atmospheric CO_2 rise and tropical warming, *Science*, *318*, 435–438.
Svensson, A., et al. (2008), A 60 000 year Greenland stratigraphic ice core chronology, *Clim. Past*, *4*(1), 47–57, doi:10.5194/cp-4-47-2008.
Thomas, A. L., G. M. Henderson, P. Deschamps, Y. Yokoyama, A. J. Mason, E. Bard, B. Hamelin, N. Durand, and G. Camoin (2009), Penultimate deglacial sea-level timing from uranium/thorium dating of Tahitian corals, *Science*, *324*, 1186–1189, doi:10.1126/science.1168754.
Thompson, W. G., and S. L. Goldstein (2006), A radiometric calibration of the SPECMAP timescale, *Quat. Sci. Rev.*, *25*, 3207–3215, doi:10.1016/j.quascirev.2006.02.007.
Thornalley, D. J. R., H. Elderfield, and I. N. McCave (2010), Intermediate and deep water paleoceanography of the northern North Atlantic over the past 21,000 years, *Paleoceanography*, *25*, PA1211, doi:10.1029/2009PA001833.
Tian, J., P. Wang, X. Cheng, and Q. Li (2002), Astronomically tuned Plio-Pleistocene benthic $\delta^{18}O$ record from South China Sea and Atlantic-Pacific comparison, *Earth Planet. Sci. Lett.*, *203*, 1015–1029, doi:10.1016/S0012-821X(02)00923-8.
Tiedemann, R., M. Sarnthein, and N. J. Shackleton (1994), Astronomic timescale for the Pliocene Atlantic $\delta^{18}O$ and dust flux records of Ocean Drilling Program site 659, *Paleoceanography*, *9*, 619–638, doi:10.1029/94PA00208.
Tjallingii, R., M. Claussen, J. W. Stuut, J. Fohlmeister, A. Jahn, T. Bickert, F. Lamy, and U. Rohl (2008), Coherent high- and low-latitude control of the northwest African hydrological balance, *Nat. Geosci.*, *1*(10), 670–675, doi:10.1038/ngeo289.
Toucanne, S., et al. (2009), Timing of massive "Fleuve Manche" discharges over the last 350 kyr: Insights into the European ice-sheet oscillations and the European drainage network from MIS 10 to 2, *Quat. Sci. Rev.*, *28*(13-14), 1238–1256, doi:10.1016/j.quascirev.2009.01.006.
Ullman, D. J., A. E. Carlson, A. N. LeGrande, F. S. Anslow, A. K. Moore, M. Caffee, K. M. Syverson, and J. M. Licciardi (2015), Southern Laurentide ice-sheet retreat synchronous with rising boreal summer insolation, *Geology*, *43*, 23–26, doi:10.1130/G36179.1.
van Kreveld, S., M. Sarnthein, H. Erlenkeuser, P. Grootes, S. Jung, M. J. Nadeau, U. Pflaumann, and A. Voelker (2000), Potential links between surging ice sheets, circulation changes, and the Dansgaard-Oeschger cycles in the Irminger Sea, 60-18 kyr, *Paleoceanography*, *15*(4), 425–442, doi:10.1029/1999PA000464.
Vautravers, M. J., N. J. Shackleton, C. Lopez-Martinez, and J. O. Grimalt (2004), Gulf stream variability during marine isotope stage 3, *Paleoceanography*, *19*, PA2011, doi:10.1029/2003PA000966.
Venz, K. A., D. A. Hodell, C. Stanton, and D. A. Warnke (1999), A 1.0 Myr record of glacial North Atlantic Intermediate Water variability from ODP Site 982 in the northeast Atlantic, *Paleoceanography*, *14*, 42–52, doi:10.1029/1998PA900013.
Veres, D., et al. (2013), The Antarctic Ice Core Chronology (AICC2012): An optimized multi-parameter and multi-site dating approach for the last 120 thousand years, *Clim. Past*, *9*, 1733–1748, doi:10.5194/cp-9-1733-2013.
Vidal, L., R. R. Schneider, O. Marchal, T. Bickert, T. F. Stocker, and G. Wefer (1999), Link between the North and South Atlantic during the Heinrich events of the last glacial period, *Clim. Dyn.*, *15*(12), 909–919, doi:10.1007/s003820050321.
Voelker, A. H. L., S. M. Lebreiro, J. Schonfeld, I. Cacho, H. Erlenkeuser, and F. Abrantes (2006), Mediterranean outflow strengthening during northern hemisphere coolings: A salt source for the glacial Atlantic?, *Earth Planet. Sci. Lett.*, *245*, 39–55.
Waddell, L. M., I. L. Hendy, T. C. Moore, and M. W. Lyle (2009), Ventilation of the abyssal Southern Ocean during the late Neogene: A new perspective from the subantarctic Pacific, *Paleoceanography*, *24*, PA3206, doi:10.1029/2008PA001661.
Waelbroeck, C., J.-C. Duplessy, E. Michel, L. Labeyrie, D. Paillard, and J. Duprat (2001), The timing of the last deglaciation in North Atlantic climate records, *Nature*, *412*(6848), 724–727, doi:10.1038/35089060.
Waelbroeck, C., C. Levi, J.-C. Duplessy, L. Labeyrie, E. Michel, E. Cortijo, F. Bassinot, and F. Guichard (2006), Distant origin of circulation changes in the Indian Ocean during the last deglaciation, *Earth Planet. Sci. Lett.*, *243*, 244–251.
Waelbroeck, C., N. Frank, J. Jouzel, F. Parrenin, V. Masson-Delmotte, and D. Genty (2008), Transferring radiometric dating of the last interglacial sea level high stand to marine and ice core records, *Earth Planet. Sci. Lett.*, *265*, 183–194, doi:10.1016/j.epsl.2007.10.006.
Waelbroeck, C., L. C. Skinner, L. Labeyrie, J.-C. Duplessy, E. Michel, N. Vazquez Riveiros, J. M. Gherardi, and F. Dewilde (2011), The timing of deglacial circulation changes in the Atlantic, *Paleoceanography*, *26*, PA3213, doi:10.1029/2010PA002007.
Wang, L., M. Sarnthein, H. Erlenkeuser, J. O. Grimalt, P. M. Grootes, S. Heilig, E. V. Ivanova, M. Kienast, C. Pelejero, and U. Pflaumann (1999), East-Asian monsoon climate during the late Pleistocene: High-resolution sediment records from the South China Sea, *Mar. Geol.*, *156*, 245–284, doi:10.1016/S0025-3227(98)00182-0.
Wang, Y. J., H. Cheng, R. L. Edwards, Z. S. An, J. Y. Wu, C.-C. Shen, and J. A. Dorale (2001), A high-resolution absolute-dated late Pleistocene monsoon record from Hulu Cave, China, *Science*, *294*, 2345–2348, doi:10.1126/science.1064618.
Wang, Y., et al. (2008), Millennial- and orbital-scale changes in the East Asian monsoon over the past 224,000 years, *Nature*, *451*, 1090–1093, doi:10.1038/nature06692.
Weaver, P. P. E., L. Carter, and H. Neil (1998), Response of surface water masses and circulation to late Quaternary climate change, east of New Zealand, *Paleoceanography*, *13*, 70–83, doi:10.1029/97PA02982.
Wei, G. J., C. Y. Huang, C. C. Wang, M. Y. Lee, and K. Y. Wei (2006), High-resolution benthic foraminifer $\delta^{13}C$ records in the South China Sea during the last 150 ka, *Mar. Geol.*, *232*, 227–235, doi:10.1016/j.margeo.2006.08.005.
Weinelt, M. (1993), Veränderungen der Oberflächenzirkulation im Europäischen Nordmeer während der letzten 60.000 Jahre - Hinweise aus stabilen Isotopen Berichte aus dem Sonderforschungsbereich 313, Christian Albrechts Univ., Kiel.
Weinelt, M., A. Rosell-Mele, U. Pflaumann, M. Sarnthein, and T. Keifer (2003), The role of productivity in the Northeast Atlantic on abrupt climate change over the last 80,000 years, *Z. Dtsch. Geol. Ges.*, *154*, 47–66.
Wells, P., and H. Okada (1997), Response of nannoplankton to major changes in sea-surface temperature and movements of hydrological fronts over Site DSDP 594 (south Chatham Rise, southeastern New Zealand), during the last 130 kyr, *Mar. Micropaleontol.*, *32*, 341–363.
Winn, K., M. Sarnthein, and H. Erlenkeuser (1991), $\delta^{18}O$ stratigraphy and chronology of Kiel sediment cores from the East Atlantic Ber. 45, Geologisch-Paläontologisches Institut und Museum, Univ. of Kiel.
Wolff, E. W., J. Chappellaz, T. Blunier, S. O. Rasmussen, and A. Svensson (2010), Millennial-scale variability during the last glacial: The ice core record, *Quat. Sci. Rev.*, *29*, 2828–2838, doi:10.1016/j.quascirev.2009.10.013.

Wood, J. R., S. L. Forman, J. Pierson, and J. Gomez (2010), New insights on Illinoian deglaciation from deposits of Glacial Lake Quincy, central Indiana, *Quat. Res.*, *73*, 374–384, doi:10.1016/j.yqres.2009.10.008.

Wu, J. Y., Y. J. Wang, H. Cheng, and R. L. Edwards (2009), An exceptionally strengthened East Asian summer monsoon event between 19.9 and 17.1 ka BP recorded in a Hulu stalagmite, *Sci. China, Ser. D: Earth Sci.*, *52*, 360–368.

Wunsch, C., and P. Heimbach (2008), How long to oceanic tracer and proxy equilibrium?, *Quat. Sci. Rev.*, *27*, 637–651.

Yamane, M. (2003), Late Quaternary variations in water mass in the Shatsky Rise area, northwest Pacific Ocean, *Mar. Micropaleontol.*, *48*, 205–223.

Yuan, D., et al. (2004), Timing, duration, and transitions of the last interglacial Asian monsoon, *Science*, *304*(5670), 575–578.

Zabel, M., T. Bickert, L. Dittert, and R. R. Haese (1999), The significance of the sedimentary Al/Ti ratio as indicator for reconstructions of the terrestrial input to the equatorial Atlantic, *Paleoceanography*, *14*, 789–799, doi:10.1029/1999PA900027.

Zahn, R., K. Winn, and M. Sarnthein (1986), Benthic foraminiferal $\delta^{13}C$ and accumulation rates of organic carbon: *Uvigerina peregrina* group and *Cibicidoides wuellerstorfi*, *Paleoceanography*, *1*, 27–42, doi:10.1029/PA001i001p00027.

Zarriess, M., and A. Mackensen (2010), The tropical rainbelt and productivity changes off northwest Africa: A 31,000-year high-resolution record, *Mar. Micropaleontol.*, *76*(3-4), 76–91, doi:10.1026/j.marmicro.2010.06.001.

Zarriess, M., and A. Mackensen (2011), Testing the impact of seasonal phytodetritus deposition on $\delta^{13}C$ of epibenthic foraminifer *Cibicidoides wuellerstorfi*: A 31,000 year high-resolution record from the northwest African continental slope, *Paleoceanography*, *26*, PA2202, doi:10.1029/2010PA001944.

Zarriess, M., H. Johnstone, M. Prange, S. Steph, J. Groeneveld, S. Mulitza, and A. Mackensen (2011), Bipolar seesaw in the northeastern tropical Atlantic during Heinrich stadials, *Geophys. Res. Lett.*, *38*, L04706, doi:10.1029/2010GL046070.

Zhang, J., P. Wang, Q. Li, X. Cheng, H. Jin, and S. Zhang (2007), Western equatorial Pacific productivity and carbonate dissolution over the last 550 kyr: Foraminiferal and nannofossil evidence from ODP Hole 807A, *Mar. Micropaleontol.*, *64*, 121–140.